

# Reconstruction of the Vertebrate Ancestral Genome Reveals Dynamic Genome Reorganization in Early Vertebrates

Yoichiro Nakatani<sup>1, #</sup>, Hiroyuki Takeda<sup>2</sup>, Yuji Kohara<sup>3</sup>, Shinichi Morishita<sup>1,4, #</sup>

<sup>1</sup> Department of Computational Biology, Graduate School of Frontier Sciences, The University of Tokyo, Kashiwa 277-0882, Japan

<sup>2</sup> Department of Biological Sciences, Graduate School of Science, The University of Tokyo, Tokyo 113-0033, Japan

<sup>3</sup> Center for Genetic Resource Information, National Institute of Genetics, Mishima 411-8540, Japan

<sup>4</sup> Bioinformatics Research and Development (BIRD), Japan Science and Technology Agency (JST), Tokyo 102-8666, Japan

<sup>#</sup> Correspondence should be addressed to Y.N. (nakatani@cb.k.u-tokyo.ac.jp) and S.M. (moris@cb.k.u-tokyo.ac.jp).

## Supplementary information

1	<i>Introduction</i> .....	1
2	<i>Identification of ohnologs and orthologs</i> .....	1
2.1	<i>Identification of vertebrate ohnologs</i> .....	1
2.2	<i>Identification of teleost ohnologs and human–medaka orthologs</i> .....	3
2.3	<i>Identification of human–chicken orthologs</i> .....	4
3	<i>Identification of conserved vertebrate linkage (CVL) blocks</i> .....	4
3.1	<i>Identification of doubly conserved synteny (DCS) blocks</i> .....	4
3.2	<i>Combining fragmented DCS blocks into CVL blocks</i> .....	5
3.3	<i>Identification of the boundaries of CVL blocks</i> .....	5
4	<i>Refinement of CVL blocks</i> .....	6
5	<i>Ancestral vertebrate and gnathostome proto-chromosomes</i> .....	7
6	<i>Ancestral osteichthyan and amniote karyotypes</i> .....	8
7	<i>Effect of changing key parameter values on reconstruction of the vertebrate ancestral genome</i> .....	8
8	<i>Phylogenetic tree of vertebrates</i> .....	9
9	<i>Supplementary figures</i> .....	10
10	<i>Supplementary tables</i> .....	59
11	<i>References</i> .....	62

## 1 Introduction

How is it possible to reconstruct ancestral vertebrate genomes without knowing the genomes of outgroup species? The fundamental principle of ancestral genome reconstruction is that the process requires three genomes, usually two descendent genomes and one outgroup genome. The three genomes do not have to be from different species. For example, extant teleost fishes have two copies of the ancestral teleost genome because of the WGD that occurred in the ancestral teleost. By comparing these two copies of the ancestral genome with the human genome, the ancestral teleost genome has been reconstructed in previous studies (Postlethwait et al. 2000; Naruse et al. 2004; Jaillon et al. 2004; Woods et al. 2005; Kohn et al. 2006). Similarly, the human genome contains four copies of the ancestral vertebrate genome produced by two rounds of WGD, which was sufficient to reconstruct the ancestral vertebrate genome at the second round of WGD. It might be difficult to reconstruct the ancestral vertebrate proto-chromosomes if numerous rearrangements occurred during the two rounds of WGD; however, in reality, only a few major interchromosomal rearrangements were observed between the two WGDs, allowing us to reconstruct the ancestral vertebrate proto-karyotype with only a few ambiguities. Alternative scenarios remained unresolved for three of the reconstructed ancestral vertebrate proto-chromosomes; nevertheless, our reconstruction was sufficient to reveal dynamic genome reorganization in early vertebrates.

## 2 Identification of ohnologs and orthologs

### 2.1 Identification of vertebrate ohnologs

Genes may be duplicated at many points in the course of evolution. The two rounds of whole-genome duplication (2R WGD) occurred after the divergence of urochordates and vertebrates, and before the divergence of ray-finned and lobe-finned fishes. Our goal was to identify ohnologs produced by 2R WGD while excluding other duplicated genes by inspecting duplication points in the phylogenetic tree. Supplementary Fig. S1A illustrates an ideal case in which the WGD events generated four and eight ohnologs in the human and medaka genomes, respectively, and all the ohnologs and their counterpart *Ciona* genes were preserved throughout evolution. The evolutionary distance between a pair of proteins is estimated by the inverse of the BLASTP raw score between the pair (Dehal et al. 2005). Assuming that recently duplicated genes are closer than pairs of older duplicates, the following properties hold in Supplementary Fig. S1A.

- The four human genes best match the same *Ciona* gene among all *Ciona* genes. Conversely, the four human genes to which the *Ciona* gene is most similar are the same four human genes. The four human genes are more similar to each other than to the *Ciona* gene because the *Ciona* gene diverged before the 2R WGD events.
- Each human gene has two orthologs in ray-finned fishes, such as medaka, that diverged after the 2R WGD events. Therefore, the human gene is closer to the ray-finned fish orthologs than to other human genes.

- None of the four human genes was copied by gene duplication after the divergence from ray-finned fishes.

These properties allow us to identify one group of four human ohnologs that corresponds to one *Ciona* gene in the ideal example in Supplementary Fig. S1A.

However, in practice, all ohnologs and their corresponding *Ciona* genes are rarely conserved due to the loss of genes, and Supplementary Fig. S1B illustrates such a difficult example. Here we show phenomena that disrupt the conservation in the order of evolution and we explain how ohnologs can be detected even in the presence of these problems.

- **Problem 1.** One serious problem is that the *Ciona* gene model is still incomplete; for example, *Ciona*-2 is unknown while the similar *Ciona*-1 gene has been sequenced, as indicated in Supplementary Fig. S1B. It then appears that the human genes numbered 1–8 best match *Ciona*-1 and are therefore assigned to a single group, even though human-1–4 and human-5–8 should have been categorized into two separate groups. To resolve this problem, we further divide the single group into subgroups so that the distance between any two genes in a subgroup is bounded by the distance between *Ciona*-1 and its best-matching human gene. This rule partitions the single group into two subgroups, correctly separating human-1–4 from human-5–8. One may be concerned that the divergence of gene evolution rates among *Ciona* genes, as well as human and medaka genes, could affect the analysis and produce false-positive groups of ohnologs. However, in the subsequent steps presented later, we will reduce the effect as possible by looking at neighboring ohnologs in synteny blocks because it is unlikely to observe a long series of erroneous ohnologs.
- **Problem 2.** Another serious problem is caused by the loss of genes. Supplementary Fig. S1B illustrates that several medaka genes were lost, making it difficult to determine that human-1 and 2 were duplicated before the split of humans and medaka. Specifically, this fact cannot be confirmed by checking that human-1 (or 2) is closer to a medaka ortholog than to human-2 because all medaka orthologs of human-1 and 2 were lost (see Supplementary Fig. S1C). This is a worst case scenario, and in most instances, we were able to recognize ohnologs by utilizing remaining medaka genes. For example, although medaka-7 was lost, we could determine that human-3 and -4 must have diverged before the split of medaka and humans because human-4 is closer to medaka-8 than to human-3. Similarly, human-8 is closer to medaka-14 than to human-7, indicating that they are ohnologs.
- **Problem 3.** The last major problem is that lineage-specific gene duplications create highly similar copies of a gene, for example, human-5 and -6 in Supplementary Fig. S1C. These duplicates are not treated as ohnologs because the distance between them is smaller than the distances to their medaka orthologs.

Based on the above findings, we implemented the steps of locating ohnolog candidates by generalizing the procedure proposed by Dehal and Boore (Dehal et al. 2005) to handle the above problems.

- **Step 1: Identification of vertebrate gene families.** Vertebrate protein sequences of human, mouse, dog,

chicken, *Tetraodon*, and *Takifugu* (version2) were obtained from Ensembl, and *Ciona* (version1) from JGI. After running an all against all BLASTP search, we used BLASTP hits with an E-value <1e-10 to identify vertebrate gene families that were expected to share common ancestral genes by categorizing vertebrate genes into distinct groups such that all genes in a group had the same best matching *Ciona* gene in terms of BLASTP raw scores. Therefore, each group had one representative *Ciona* gene at this point. However, to cope with Problem 1, each group was further divided, ensuring that the distance between any two genes in different subgroups was larger than the distance between the representative *Ciona* gene and its best-matching human gene in the group.

- **Step 2: Extraction of ohnologs created by 2R WGD from vertebrate gene families.** Individual vertebrate gene families should include ohnologs created by 2R WGD before the split of ray-finned and lobe-finned fishes, but they may also contain duplicated genes copied recently in particular lineages. To eliminate the latter class of lineage-specific duplicates, any two human genes were not considered ohnologous if they were closer to each other than to any medaka gene, which implied that they were copied after the medaka–human divergence. In addition to such non-ohnologous genes, we found that some groups contained numerous human genes generated by both gene duplications and the 2R WGD. Because it was difficult to distinguish ohnologs created solely by the 2R WGD process from others created the combined processes, we used only groups that included at most four duplicated human genes before the divergence of ray-finned and lobe-finned fishes, and treated human genes with no duplication after the divergence of ray-finned and lobe-finned fishes as ohnologs.

Considering the incompleteness of the *Ciona* genome, we also conducted the analysis described above using the sea urchin as an outgroup instead of *Ciona*, and combined the two ohnolog candidate sets. The collected ohnolog candidates are displayed along the individual human chromosomes in Supplementary Fig. S2. Our analysis essentially followed the method of Dehal and Boore (Dehal et al. 2005), and these two methods produced almost consistent paralogous regions across human chromosomes. We also compared several other methods developed in previous studies (Dehal et al. 2005; Dehal et al. 2006; Blomme et al. 2006) and found that phylogenetic tree construction was efficient in reducing erroneous identification of ohnologs; however, it also reduced the number of identified ohnologs among paralogous chromosomal regions. Since we developed a statistical reconstruction method that was robust against erroneously identified ohnologs, we omitted phylogenetic tree analysis to obtain a better reconstruction result as a whole.

## 2.2 Identification of teleost ohnologs and human–medaka orthologs

Following the procedure outlined in the previous section for detecting ohnologous human genes created by the 2R WGD, we attempted to identify ohnologous medaka genes created in the teleost WGD event. For this purpose, we used human genes as the outgroup, replacing *Ciona* genes, and we utilized pufferfish genes to test whether a pair of medaka genes were ohnologs or the result of gene duplication after the split of medaka and pufferfish. In Step 1, considering the substantial collection of human genes, which contrasted sharply

with the partial collection of *Ciona* genes, we categorized teleost genes into one group if they were best-matched with the same human gene. From a group of medaka genes, the gene with the highest similarity score to the outgroup human gene was selected as a representative. The representative gene qualified as a medaka ortholog for the outgroup human gene if the medaka genes in a group had at most one duplication event before the divergence of medaka and pufferfish. These medaka orthologs are also juxtaposed along the human chromosomes at the bottom of Supplementary Fig. S2.

### 2.3 Identification of human–chicken orthologs

Any human and chicken genes were orthologous if they were reciprocal best matches and neither of them had teleost genes with a higher similarity score. The chicken ortholog genes are also plotted in Supplementary Fig. S2.

## 3 Identification of conserved vertebrate linkage (CVL) blocks

Chromosomal segments in the vertebrate ancestor are distributed throughout the human genome due to intensive interchromosomal rearrangements (see Fig. 1). However, few interchromosomal rearrangements took place in the teleost lineages after the teleost WGD (Postlethwait et al. 2000; Naruse et al. 2004; Jaillon et al. 2004). Thus, although chromosomal segments in the vertebrate ancestor may have been broken into smaller segments and distributed over the human genome, their counterparts are likely to be highly preserved in the two (or three due to some chromosomal fissions) medaka chromosomes that were derived from the same chromosome in the ancestral teleost karyotype. Therefore, for detecting conserved vertebrate linkage (CVL) blocks, we attempted to identify blocks of human genes that had medaka orthologs on medaka chromosomes originating from the same chromosome in the ancestral teleost karyotype.

### 3.1 Identification of doubly conserved synteny (DCS) blocks

To this end, in the initial step, we utilized doubly conserved synteny (DCS) (Kellis et al. 2004; Jaillon et al. 2004) and identified the correspondence between human genes on one human chromosome and medaka orthologs on two duplicated medaka chromosomes by comparing the medaka and human genomes. Supplementary Fig. S3 summarizes the result. Some small DCS regions were added by manual inspection, but the ancestral teleost karyotype was unchanged. DCS is useful in providing an overview of correspondence between human and medaka chromosomes. For example, in Supplementary Fig. 2, human chromosome 1 has three major distinct DCS correspondences with the medaka genome, namely, medaka chromosomes 17-4, 5-7, and 11-16 (medaka chromosomes 11 and 22 also has a DCS correspondence as indicated in Supplementary Fig. S2, which is estimated to be a result of a translocation from 16 to 22 after the teleost WGD event). DCS does not immediately indicate CVL blocks; Supplementary Fig. 2 shows that each DCS region is not consecutive on human chromosome 1, but is partitioned into smaller blocks, and these

blocks should be recognized as CVL blocks.

### 3.2 Combining fragmented DCS blocks into CVL blocks

In principle, DCS regions should be divided if interrupted by inversions or translocations in the human lineage. However, DCS blocks are frequently fragmented into smaller blocks by translocations after the teleost WGD event in the medaka lineage. Here, we illustrate this problem, and afterwards we will present a solution to it. Supplementary Fig. S4A shows an ideal case for CVL block construction. In the green region of HSA6, most of the human genes are syntenic to the reconstructed teleost ancestor chromosome TEL-a because their medaka orthologs are found in its daughter chromosomes OLA22 and OLA24. This region constitutes one CVL block because it is not interrupted. However, interchromosomal translocations in the medaka lineage create some problems, and Supplementary Fig. S4B illustrates the effect of translocation in the medaka lineage. The four yellow genes were originally located in chromosome TEL-a of the teleost ancestor, but were translocated from OLA22 to OLA16 after WGD. Because of this translocation, the yellow human genes in the green region of HSA6 have medaka orthologs in OLA16 and were erroneously assigned to TEL-b. In this case, teleost ancestor synteny in the green region is interrupted by yellow genes even though the green region should be treated as one CVL block because it has no major rearrangements in the human lineage. Therefore, in the construction of CVL blocks, we need to let a small number of genes break into other CVL blocks to avoid partitioning them into smaller parts. However, allowing too many such synteny-interrupting genes may result in the merging of two unrelated CVL blocks.

To decide how many synteny-interrupting genes should be permitted, we investigated the size distribution of contiguous human genes that had orthologs on the same medaka chromosome (Supplementary Fig. S4C), observing that 4336 of 4356 contiguous synteny regions were smaller than 10 genes in size. A threshold smaller than 10 genes was likely to divide DCS regions into too many smaller CVL blocks, while a larger threshold often failed to identify small CVL blocks inside DCS regions. Therefore, we decided to divide a DCS region into two blocks if two proximate human genes in the DCS region were interrupted by at least 10 genes belonging to different DCS regions, e.g., in Supplementary Fig. S4B, the green region becomes one CVL block because the maximum size of contiguous synteny-interrupting genes is two. If the interrupting region with at least 10 genes is a DCS region, it is treated as a single CVL block as illustrated in Supplementary Fig. S5A. Stated another way, the minimum number of genes in a CVL block is set to ten. One may wonder how the reconstruction is affected if the minimum threshold is changed. We will discuss this issue later.

### 3.3 Identification of the boundaries of CVL blocks

After the division into CVL blocks, the boundary between neighboring CVL blocks was not always clear; rather, two neighboring blocks often overlapped and some genes were mixed in the boundary region (Supplementary Fig. S5A). Furthermore, many genes (depicted as white boxes) did not have orthologs in the

medaka genome probably because counterpart genomic regions were deleted, or massive mutations produced pseudogenes or genes of different functions. We considered putting unassigned genes surrounded by a pair of “assigned” genes on a CVL block into the same CVL block, but the region between the pair could contain some genes associated with teleost ancestor chromosomes other than that of the CVL block, as well as unassigned genes. To properly eliminate this noise, we applied the condition that the unassigned genes are put into the CVL block if the region involves only unassigned genes except for at most one gene assigned to a medaka ortholog that is not mapped to any teleost ancestor chromosome. The exception was tolerated because about 90% of the medaka genome is covered by mapped scaffolds, and small-scale interchromosomal translocations in the medaka lineage may have put such an unassigned gene into the CVL.

## 4 Refinement of CVL blocks

Here we discuss a serious issue that may arise during the construction of CVL blocks, and we present a solution to the problem. The major problems in the reconstruction of CVL blocks are genome rearrangements that took place after the 2R WGD in the ancestral vertebrate genome and before the divergence of ray-finned and lobe-finned fishes. If the genome of a cartilaginous fish were available, it would provide valuable information to resolve this problem. These rearrangements are still present in the human and fish genomes, making it difficult to reconstruct the ancestral vertebrate proto-karyotype. Supplementary Fig. S6A illustrates two fission events that took place prior to the osteichthyan ancestor. The four chromosomal fragments originating from these fissions survived as CVL blocks, and CVL blocks derived from the same vertebrate proto-chromosome are correctly assigned to one connected component in the CVL graph. Then, these blocks are combined into ancestral gnathostome chromosomes as described in the Methods section of the main text. For example, B4L have many common ohnologs with BL1 as well as B1R, but it shares none with B4R, indicating that a fission event break one proto-chromosome into B4L and B4R. In this case, no need exists to refine the CVL blocks.

However, chromosomal fusions that occurred before the osteichthyan ancestor are likely to have serious consequences, that is, undesirable CVL blocks with two fragments originating from multiple distinct proto-chromosomes, as shown in Supplementary Fig. S6B. Such unqualified CVL blocks could also be produced by numerous chromosomal rearrangements occurring independently in distinct ray-finned and lobe-finned fish lineages (Supplementary Fig. S6C). Creating such improper CVL blocks should be avoided, but they can only be detected after the reconstruction of the ancestral vertebrate karyotype by checking whether they have a significantly great amount of ohnologs in more than one vertebrate proto-chromosome. Supplementary Fig. S6D illustrates how CVL block A4+B1L can be identified as a fused CVL block. In this case, CVL block A4+B1L is paralogous to A1, A2, and A3, so it is assigned to the red connected component. Since the B1L region has few ohnologs in A1–A3, but several ohnologs in B2–B4L, the B1L region can be identified by mapping red and green ohnologs to CVL block A4+B1L. Specifically, each CVL block is checked for whether ohnologs from two connected components are distributed nonrandomly over the CVL

block by conducting a Mann–Whitney *U*-test. If the two-tailed probability is  $<0.01$ , the CVL block is divided into two blocks. For example, in Supplementary Fig. S6D, genes between two red ohnologs that are not interrupted by green ohnologs are assigned to new CVL block, and vertebrate proto-chromosomes can be reconstructed correctly.

Supplementary Fig. S6E shows a more complicated case of fused CVL blocks, in which A4+B1L is paralogous to red and green CVL blocks, and one large connected component corresponding to two ancestral vertebrate proto-chromosomes is obtained. In this case, CVL block A4+B1L cannot be identified as a fused CVL block as in Supplementary Fig. S6D because A4 and B1L have ohnologs in the same connected component. To avoid making such erroneous connected components, we checked whether a connected component can be divided into two subcomponents that share significantly fewer ohnologs. If the probability of finding fewer ohnologs by chance (see Methods) was less than 0.01 (this parameter value did not affect the result if it is changed to 0.1 or 0.001), the CVL block was identified as a fused CVL block and its edges were removed from the CVL graph except for the edge to the most significantly paralogous CVL block. Subsequently, we conducted the CVL block refinement step in Supplementary Fig. S6D. In our analysis, for example, CVL block #63 was identified as a fused CVL block, and divided into new CVL blocks #63 and #113. This division is validated independently by chicken synteny since CVL blocks #63 and #113 have orthologs in different chicken chromosomes (see Supplementary Fig. S2, human chromosome 11). After dividing the CVL blocks, we constructed CVL graphs and reconstructed ancestral vertebrate proto-chromosomes.

In the initial step, 109 CVL blocks were generated, and subsequently, the refinement process produced a total of 118 CVL blocks. Striking examples can be seen in human chromosome 17, in which CVL blocks #82 and #84 were divided into two parts that were consistent with the break points of human–chicken synteny (Supplementary Fig. S2, human chromosome 17).

## 5 Ancestral vertebrate and gnathostome proto-chromosomes

Reconstructed ancestral vertebrate proto-chromosomes are listed in Supplementary Fig. S7. For each ancestral vertebrate proto-chromosome, the most significant five reconstruction candidates are shown at the top of the table; the left column indicates significance in terms of probability and the remaining columns indicate CVL blocks constituting individual sister chromosomes. In the Methods of the main text, we have described how to compute the significance of reconstructed gnathostome proto-chromosomes in order to select the optimum one.

Reconstruction using CVL blocks with a smaller number of genes is less reliable than using larger CVL blocks, which makes it difficult to rebuild smaller proto-chromosomes. In contrast, larger proto-chromosomes with more ohnologs are more reliable. One effective way to reconfirm the reconstruction is to examine how CVL blocks in one proto-chromosome are clustered in the ancestral teleost karyotype and the chicken genome. For example, the largest sister chromosome of proto-chromosome C consists of seven

CVL blocks and all of the blocks are in the same teleost ancestor chromosome k and chicken chromosome 1, supporting the ancestral linkage of the seven CVL blocks.

## 6 Ancestral osteichthyan and amniote karyotypes

In the reconstruction of osteichthyan and amniote ancestors, synteny regions in the chicken genome for CVL blocks must be identified. We joined the genes constituting a CVL block into synteny blocks by applying Bourque *et al.*'s "gene7" method (Bourque et al. 2005) with an additional restriction that synteny blocks should not be extended outside of the CVL block. Specifically, we joined two orthologs in a CVL block if they satisfy the conditions of "gene7."

"Two genes A and B are joined together if there are up to two intervening genes between them in every species, with certain constraints on flipping A and B: at two intervening genes, the relative orientations of A and B must be the same in all species or one of them can be flipped, and with less than two intervening genes, either or both can be flipped. Next, we discarded blocks supported by less than three genes." (Bourque et al. 2005)

Then, we applied the 2-of-3 rule to reconstruct the ancestral chromosomes. CVL blocks in the chromosomes of vertebrate, osteichthyan, and amniote ancestors, and synteny block size between CVL blocks and chicken chromosomes are listed in Supplementary Tables S1–S3.

## 7 Effect of changing key parameter values on reconstruction of the vertebrate ancestral genome

The following three parameters are essential to reconstruct CVL blocks and the vertebrate ancestral genome:

1. the threshold on the number of genes in a CVL block (see Subsection 3.2 in the supplementary document),
2. the significance threshold for testing if two CVL blocks are paralogous (see Methods in the main text), and
3. the significance threshold for the Mann-Whitney U-test to decide whether a CVL block is divided (see Section 4 in the supplementary document).

The default values of individual parameters are 10, 1E-4, and 1E-2, respectively. To see the effect of these parameters on our analysis, we reconstructed the vertebrate ancestral genome with parameter values that were lower or higher than the default values. Supplementary Table S4 presents the results when the first parameter is set to 7, 10 and 13, the second parameter to 5E-4, 1E-4 and 5E-5, and the third parameter to 5E-2, 1E-2 and 1E-3. Although the number of CVL blocks is somewhat affected by the change of parameter values, the numbers of vertebrate groups (or, proto-chromosomes) in vertebrate, gnathostome, osteichthyan, and

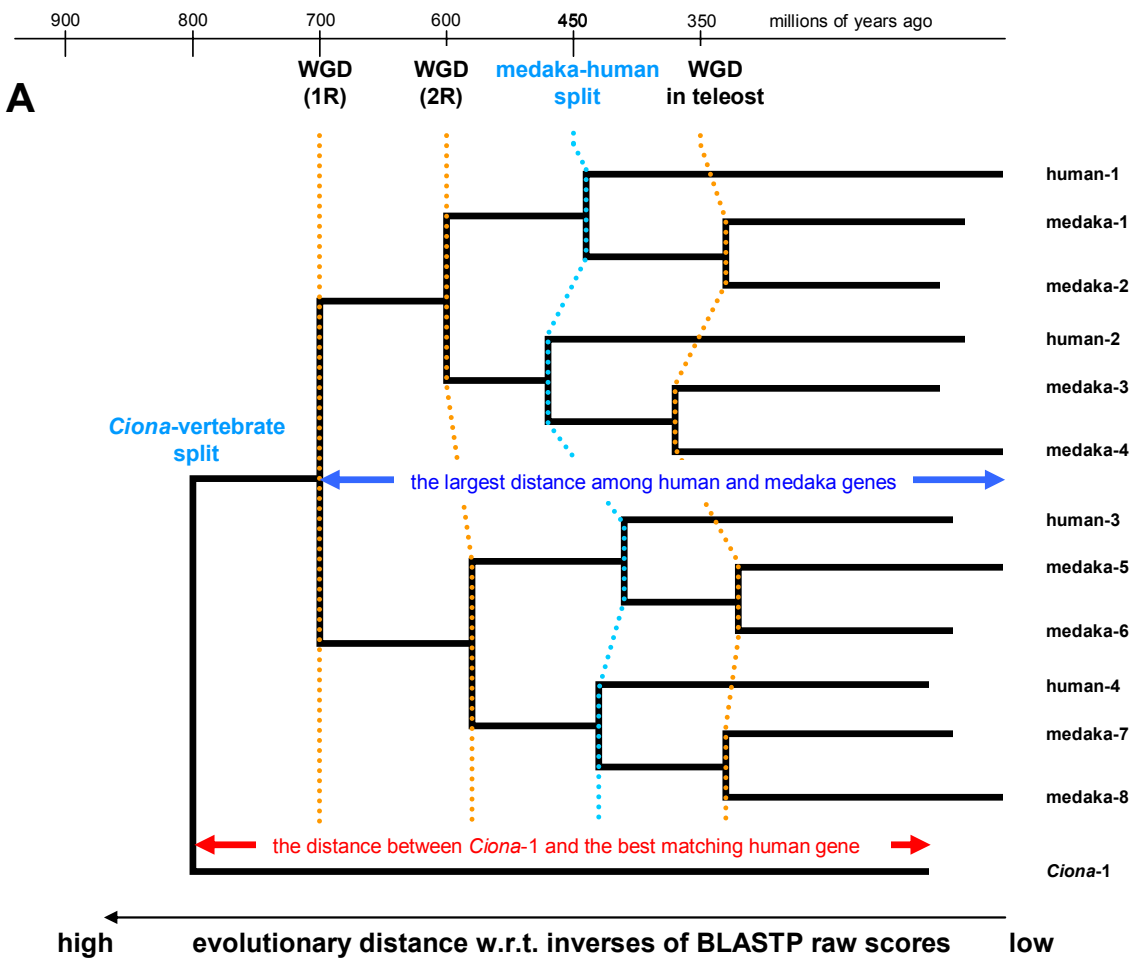
amniote ancestors are almost stable and are consistent with respective numbers in the default setting of parameters, thereby reconfirming our scenario of karyotype evolution. Minor changes are observed in Cases 3, 4, and 6. In Case 3, the first parameter is set to 13, which is higher than the default value 10. The setting is likely to merge fragmented DCS blocks into CVL blocks, producing five gnathostome proto-chromosomes for vertebrate proto-chromosome C. In Cases 4 and 6, the vertebrate proto-chromosomes C and F are fused into one.

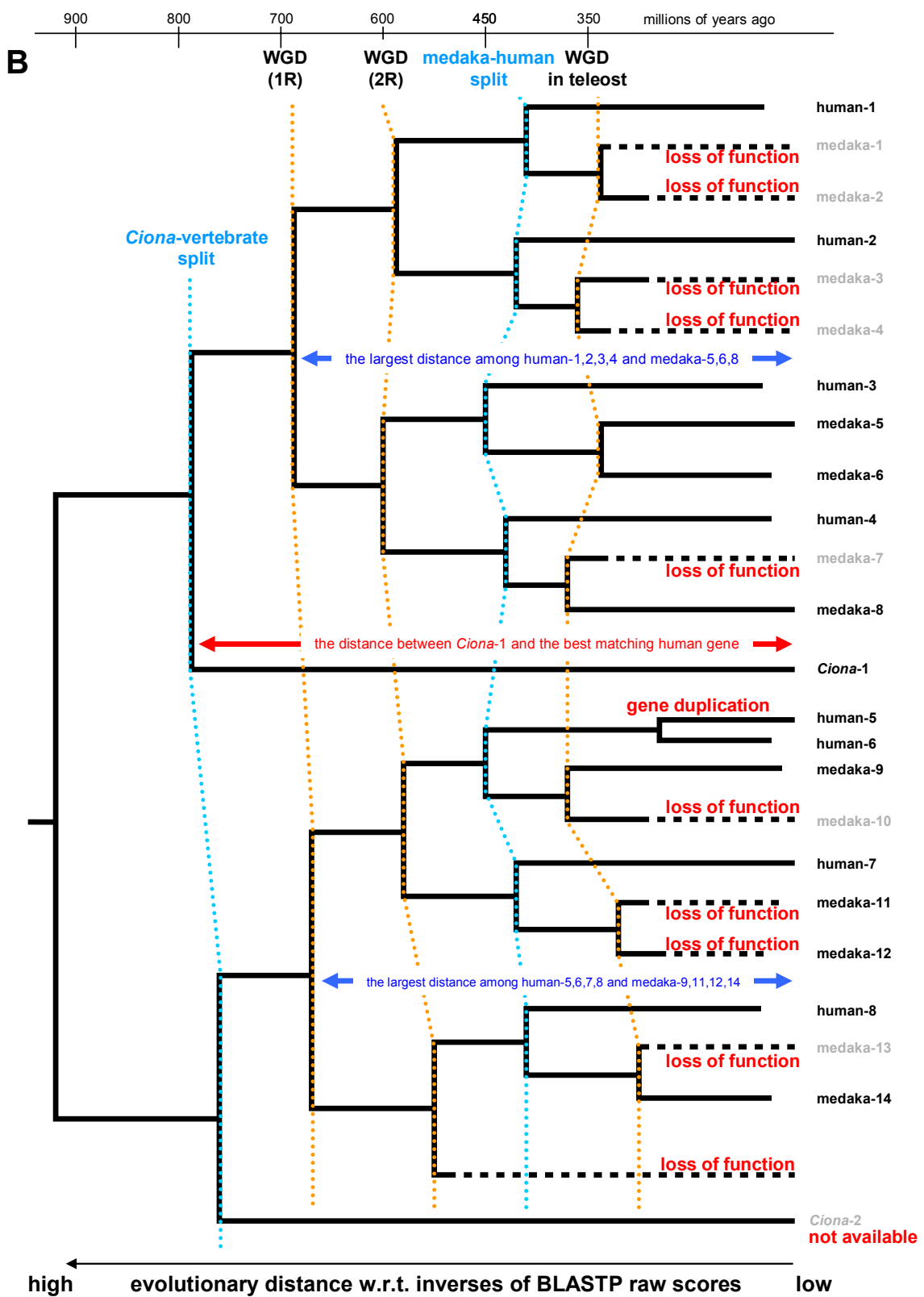
## 8 Phylogenetic tree of vertebrates

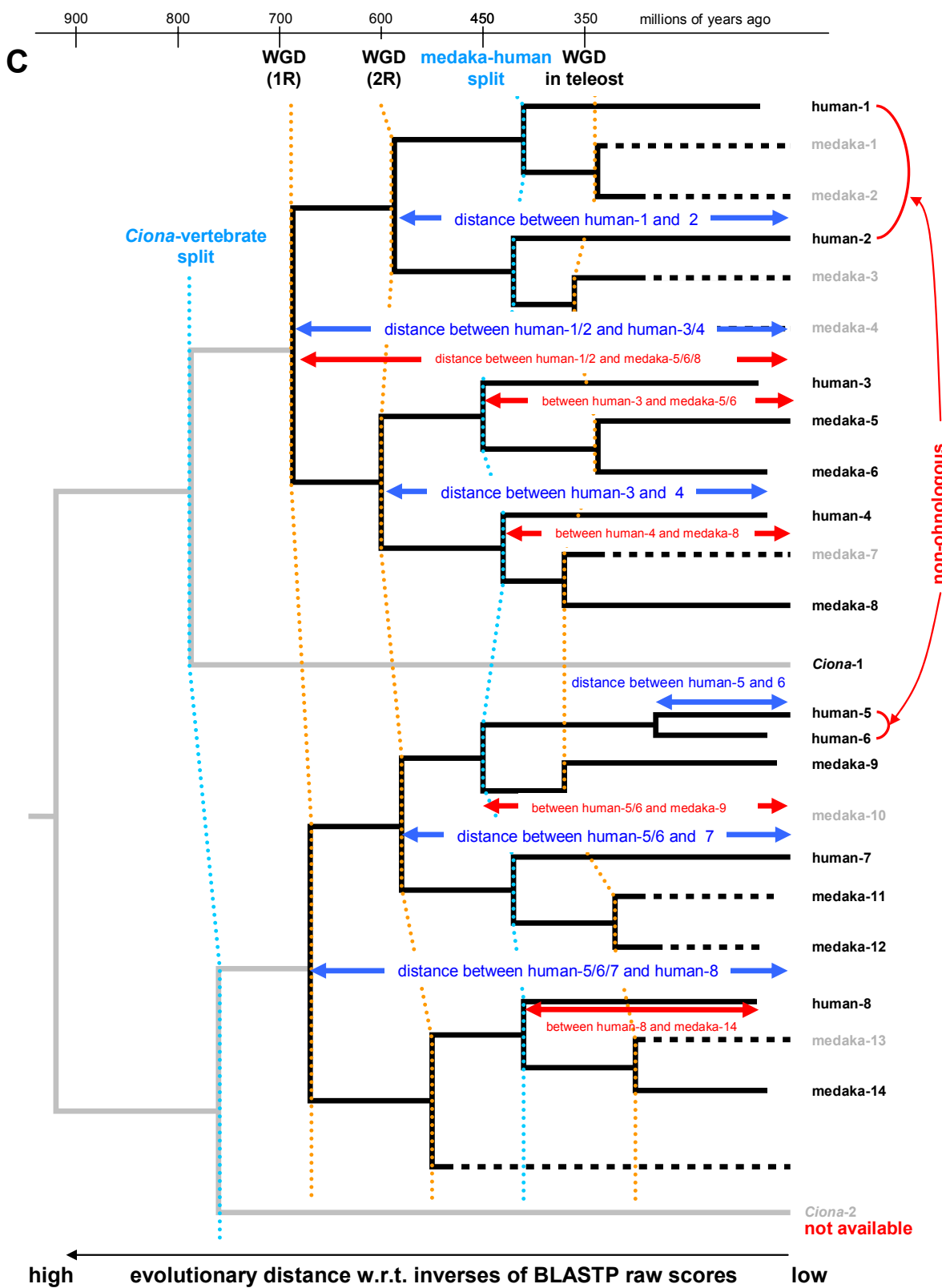
The phylogenetic tree in Fig. 6 is based on information presented in previous reports. We referred to Yamanoue *et al.* (Yamanoue *et al.* 2006) for the divergence times of torafugu, spotted green pufferfish, medaka, zebrafish, and the sarcopterygian–actinopterygian split, and to Inoue *et al.* (Inoue *et al.* 2005) for the divergence times of bichir, sturgeon, paddlefish, gar, and bowfin. We referred to Hedges and Poling (Hedges *et al.* 1999) for Reptilia, to Woodburne *et al.* (Woodburne *et al.* 2003) for Monotremata and Metatheria, to Springer *et al.* (Springer *et al.* 2003) for Mammalia, and to Blair and Hedges (Blair *et al.* 2005) for the rest, although some of the phylogenetic relationships and divergence times presented remain controversial (Meyer *et al.* 2003; Benton *et al.* 2007). The phylogenetic timing of the two rounds of whole-genome duplication in the vertebrate ancestor is cited from Stadler *et al.* (Stadler *et al.* 2004) and in the teleost ancestor, Hoegg *et al.* (Hoegg *et al.* 2004) and Crow *et al.* (Crow *et al.* 2006). The right column in Fig. 4 shows distributions of chromosome numbers up to  $2n=100$ ; some species have more chromosomes, but were not included because of space limitations. Supplementary Fig. S8 shows the complete distributions. Chromosome number data were obtained from the Animal Genome Size Database [Gregory (2006): <http://www.genomesize.com>].

## 9 Supplementary figures

Supplementary Figure S1



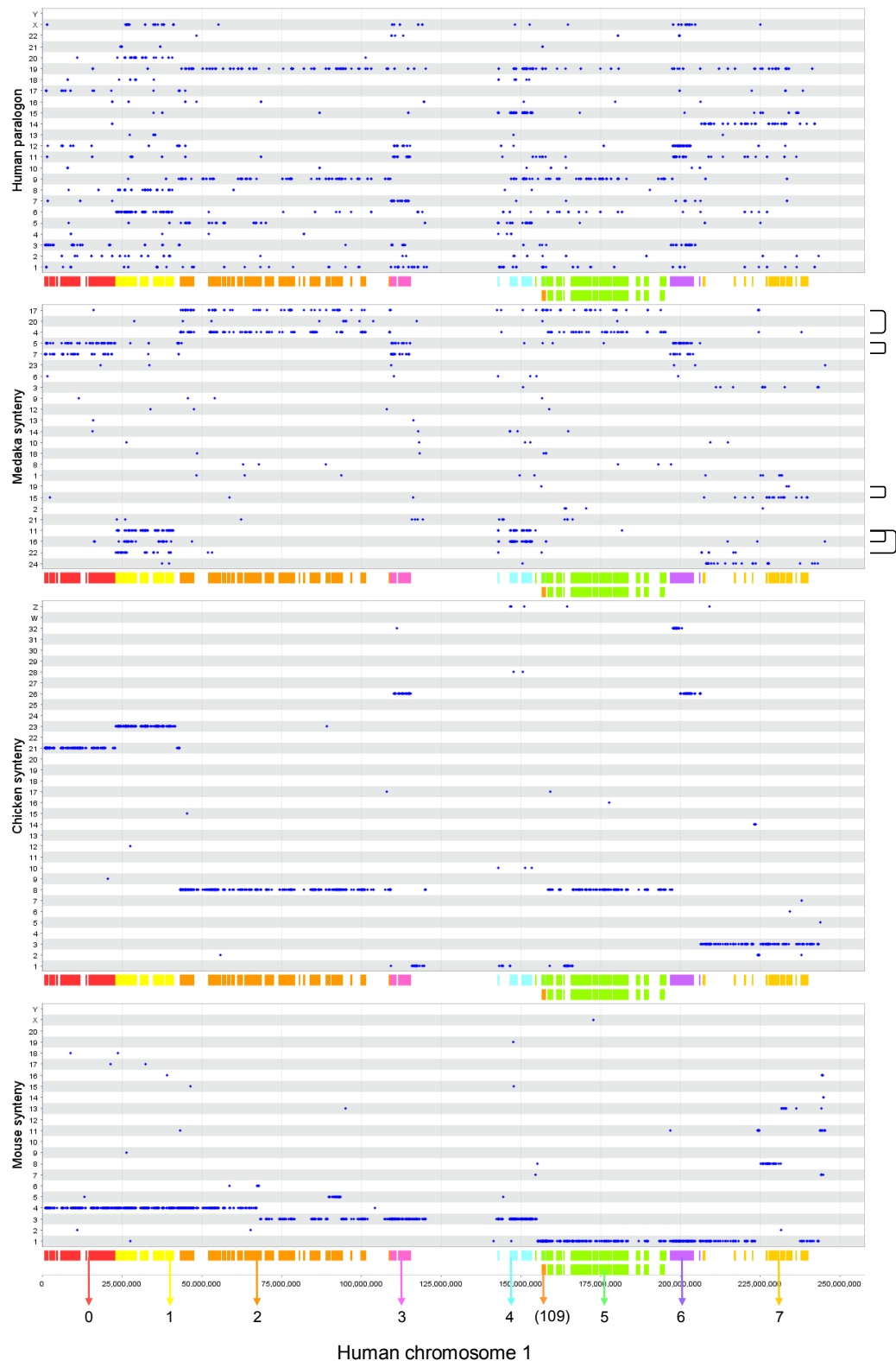


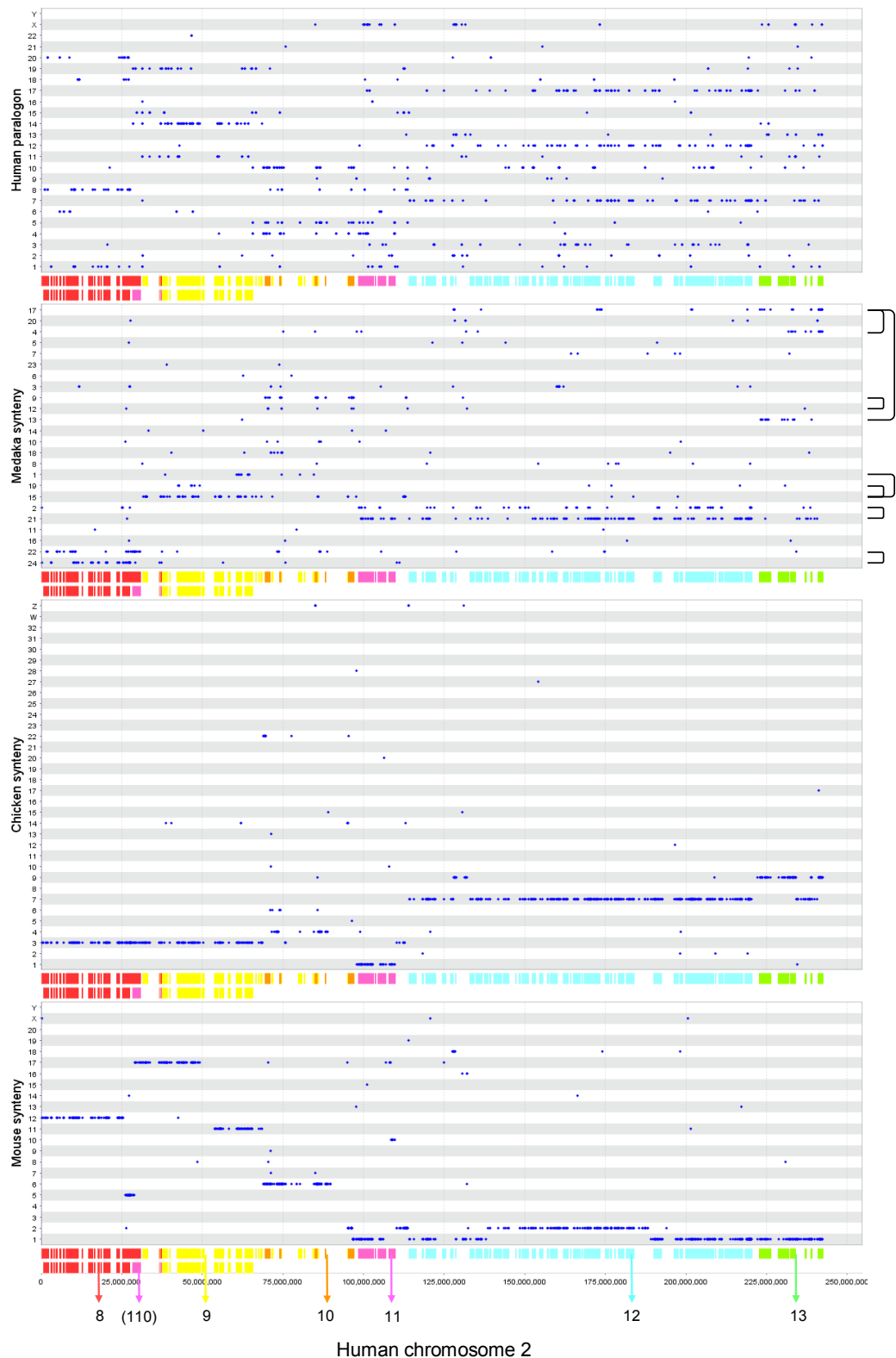


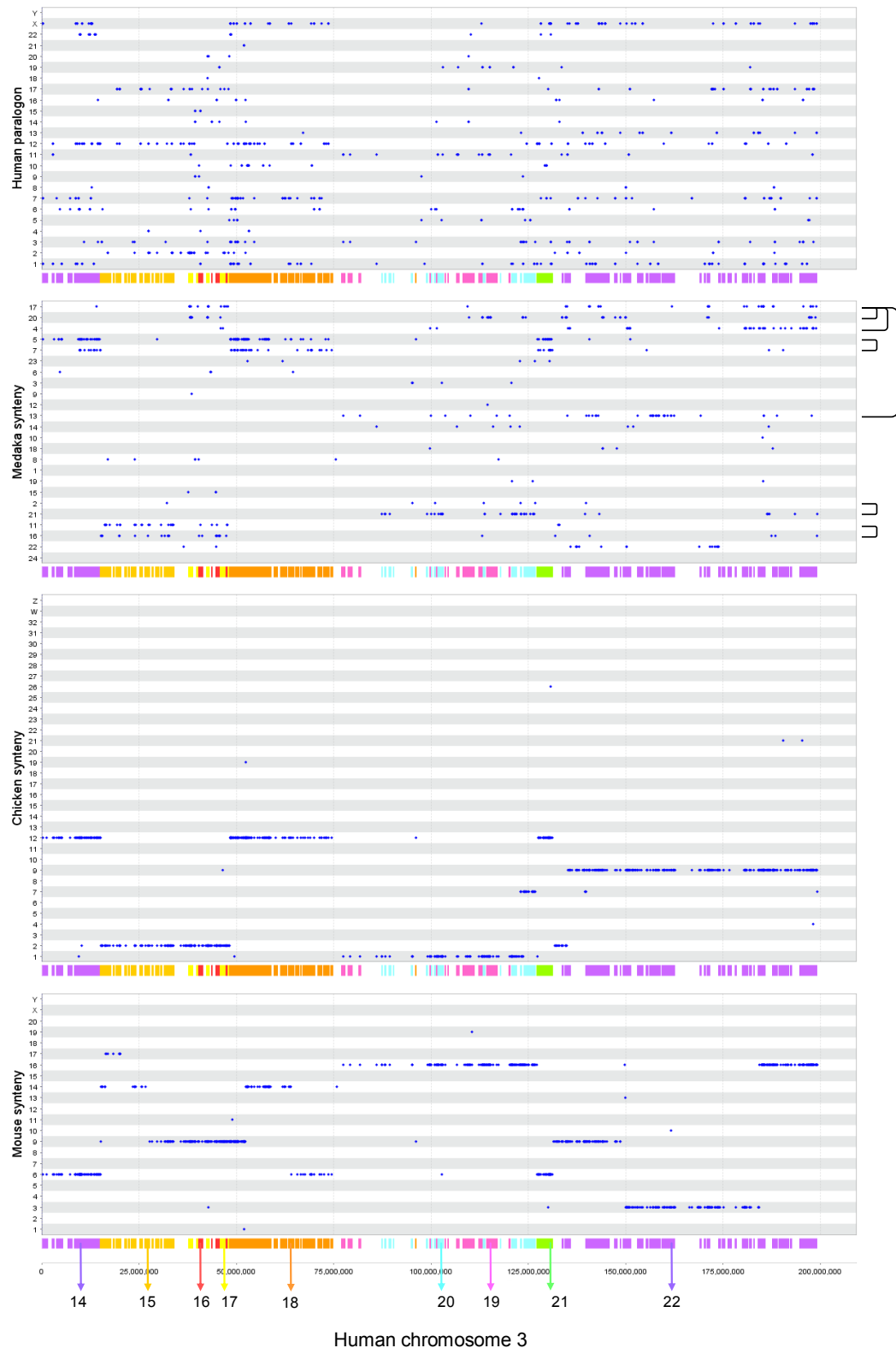
**Phylogenetic tree of human, medaka, and *Ciona* genes.** Evolutionary distances were calculated as inverses of BLASTP raw scores between pairs of two genes. **A.** The two rounds of whole genome duplication events in the vertebrate ancestor and the teleost whole genome duplication generated four human and eight medaka ohnologs. **B.** Several medaka genes were lost in the medaka lineage, one chromosome was lost before the medaka-human split, and *Ciona*-2 has not yet been sequenced. All human and medaka genes were most similar to *Ciona*-1 and were therefore temporarily categorized into one group. **C.** This temporary group was divided into two subgroups generated after the *Ciona*–vertebrate split such that the distance between any genes in individual subgroups is bounded by the distance between *Ciona*-1 and the best matching human gene.

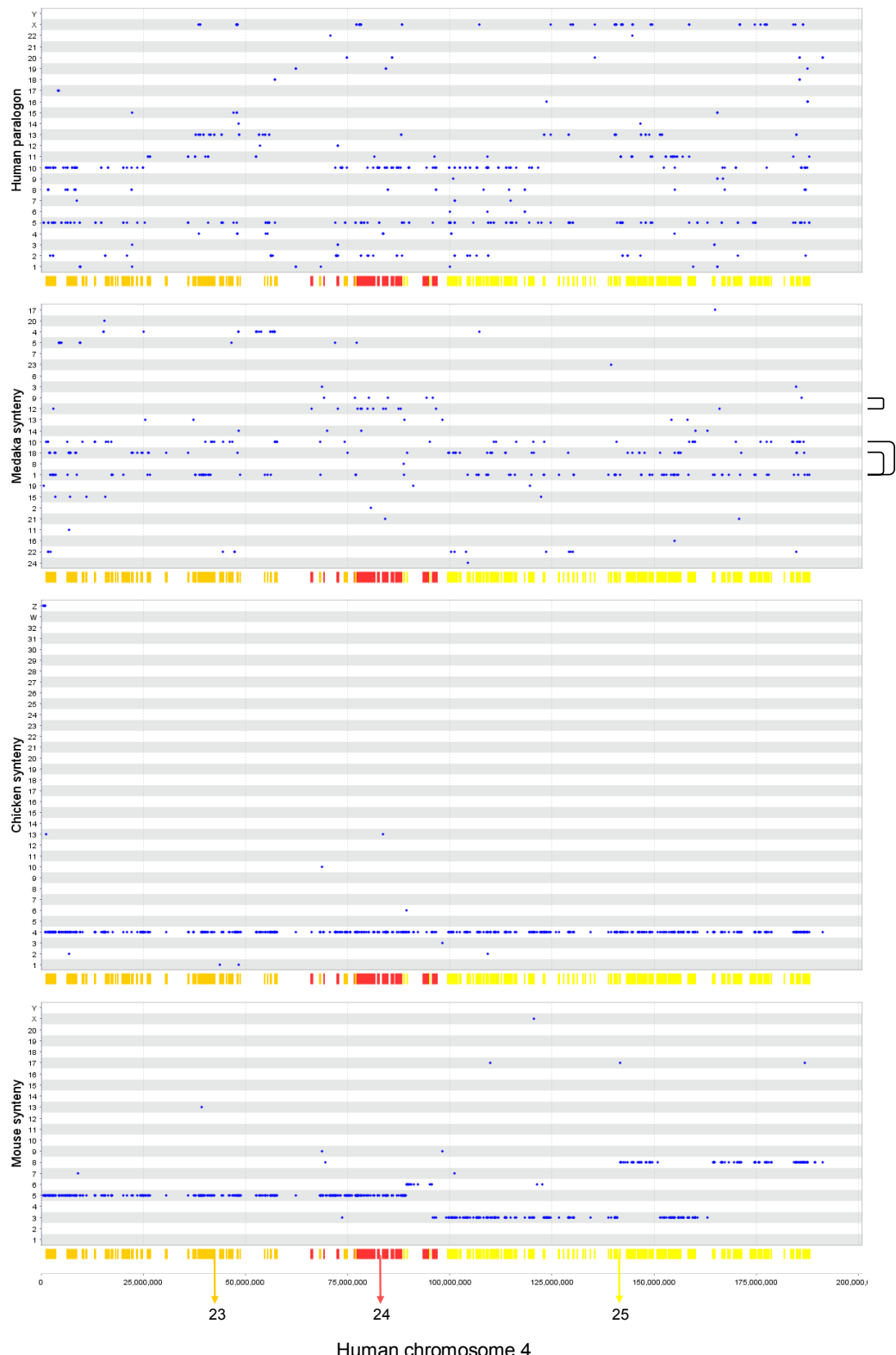
## Supplementary Figure S2

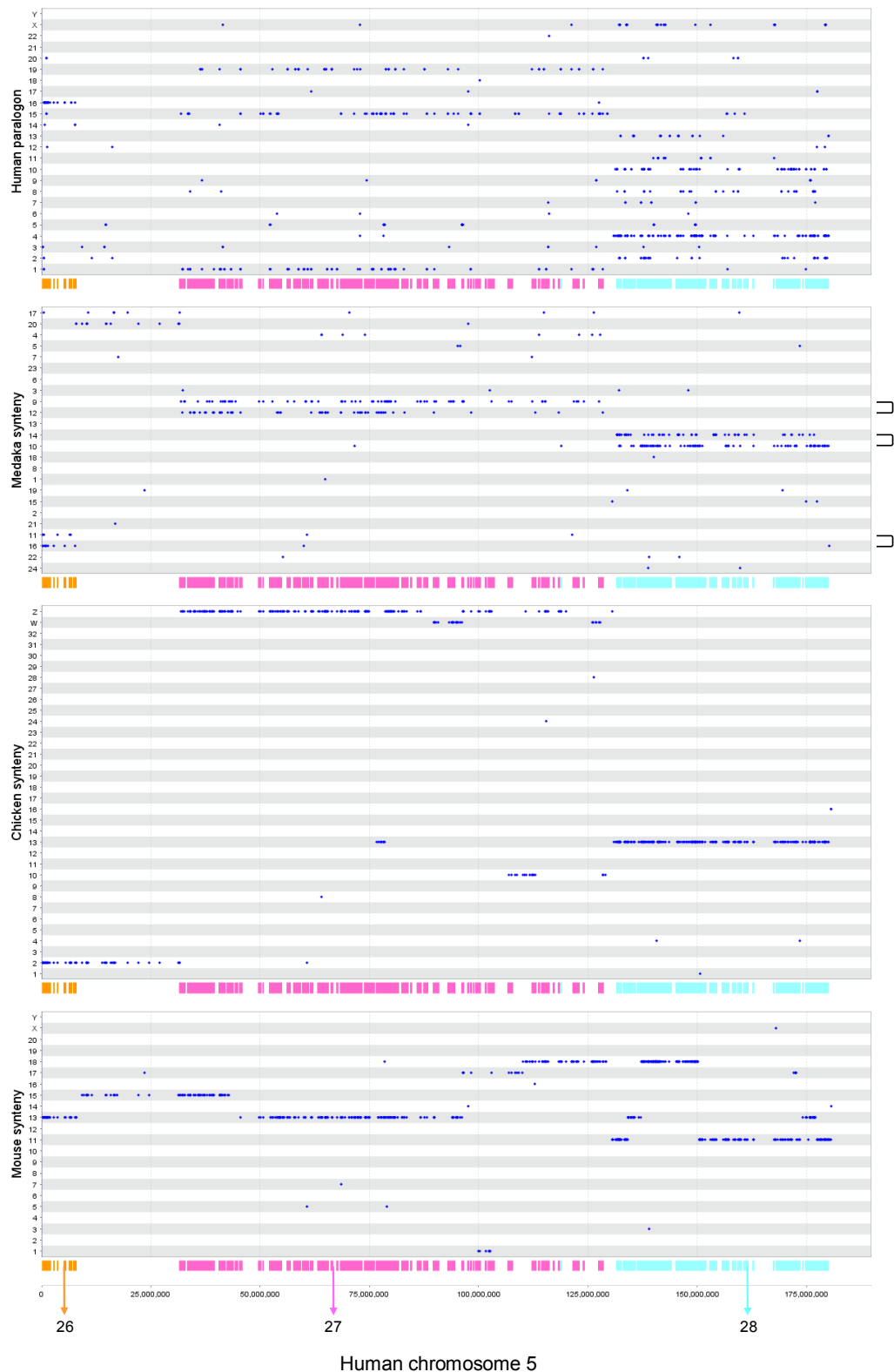
**Human ohnlogs and orthologs of medaka, chicken, and mouse.** Genes in one CVL block have the same color. CVL blocks in the upper row indicate the original 109 blocks (see “Identification of CVL blocks”), while those in the lower row, indicate the refined blocks (see “Refinement of CVL blocks”). These blocks are displayed along individual human chromosomes from the p to the q telomere and are numbered from 0 to 117. Those numbered from 109 to 117 were isolated in the CVL block refinement step, and these numbers are enclosed in parentheses to highlight this modification. Duplicated medaka chromosome pairs are connected by lines on the right side of the medaka ortholog plot.

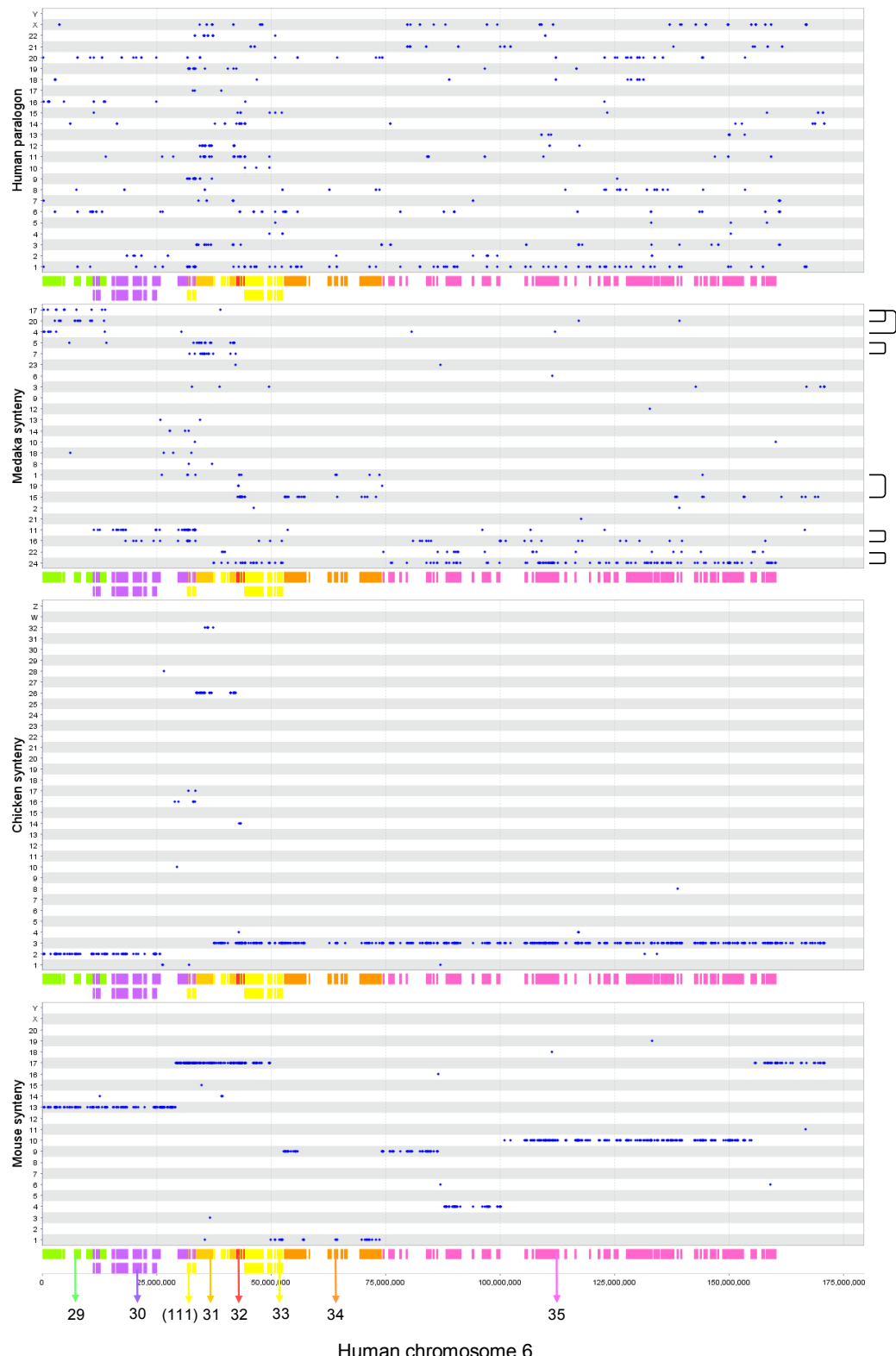


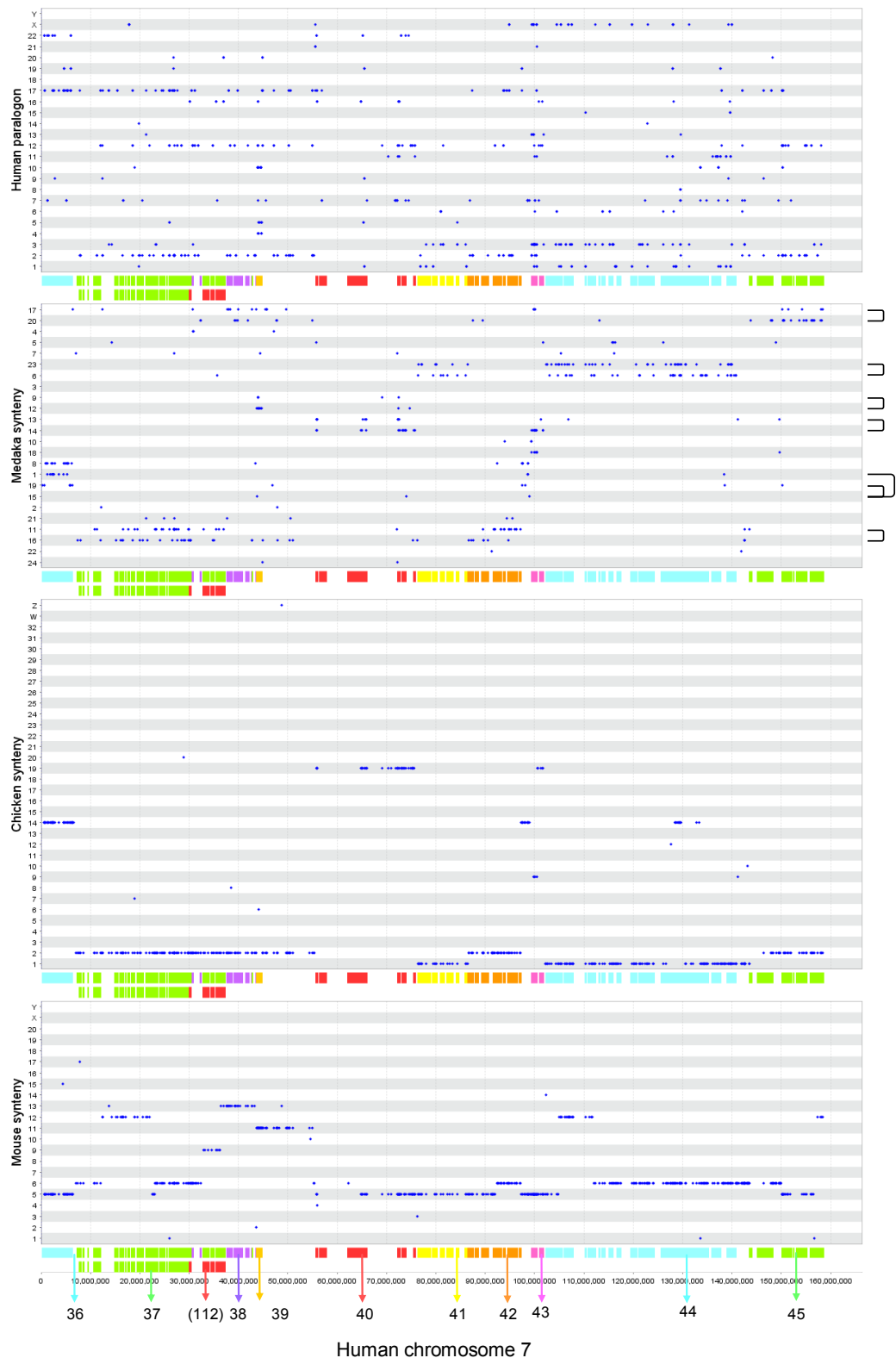


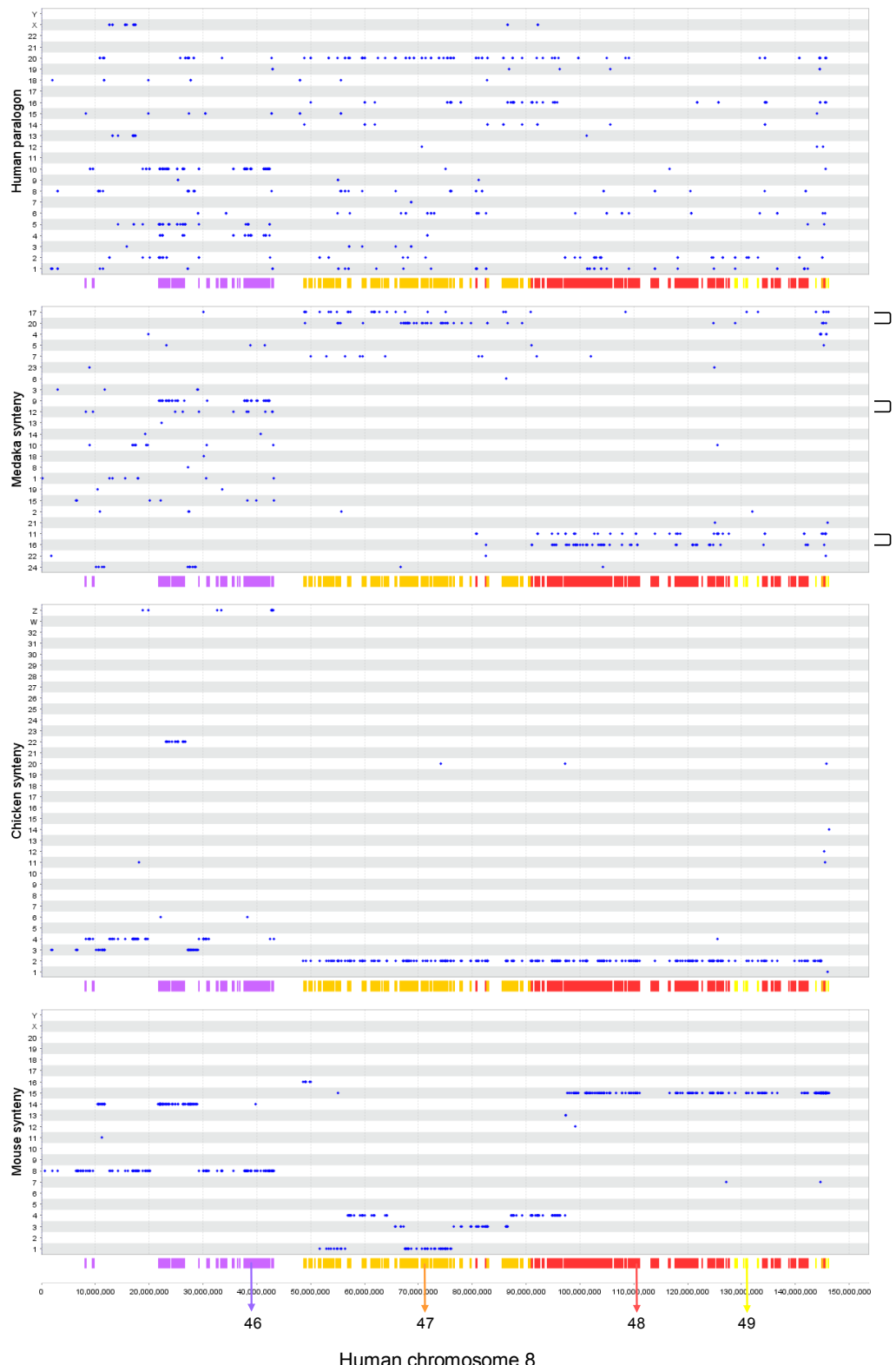


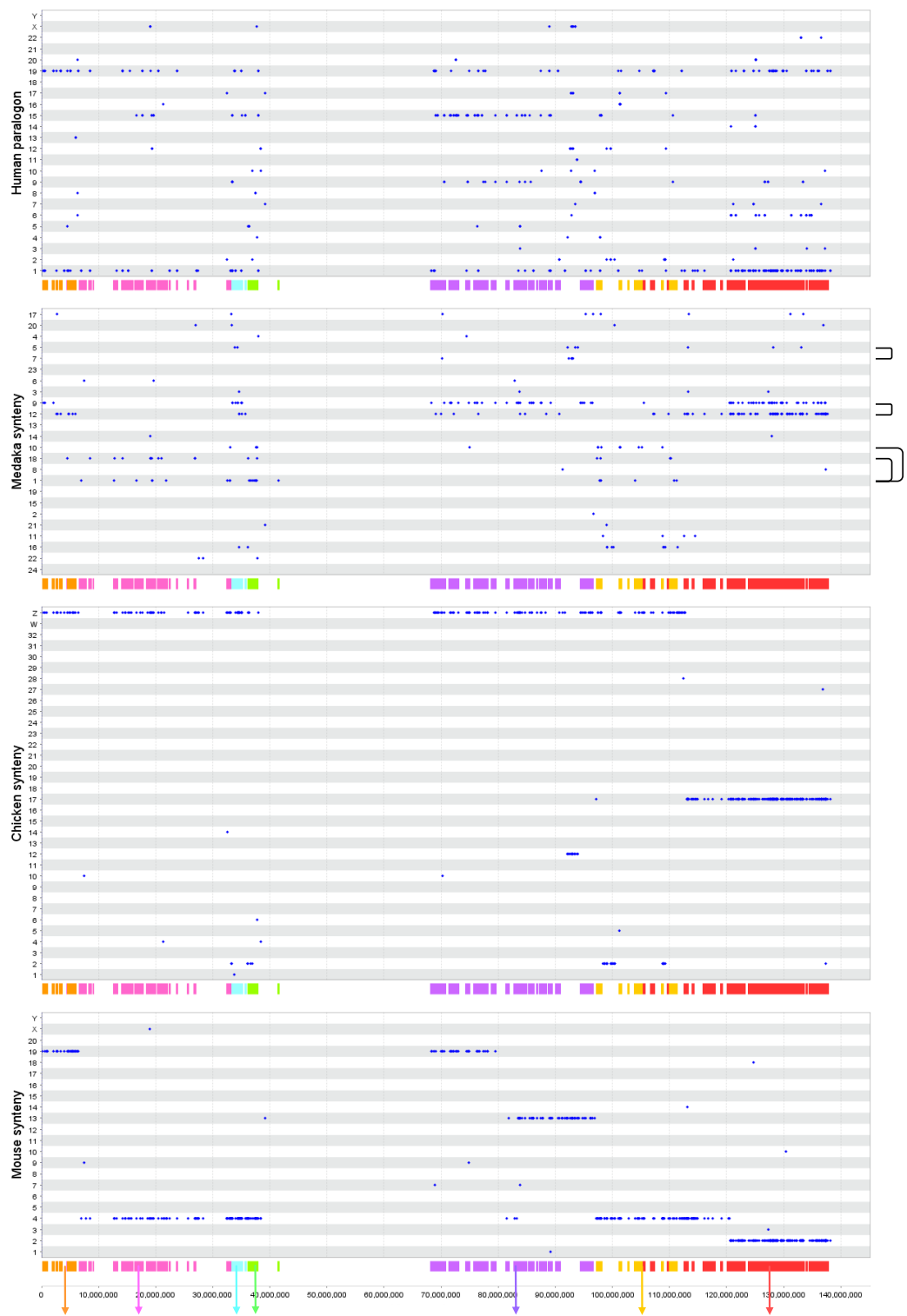


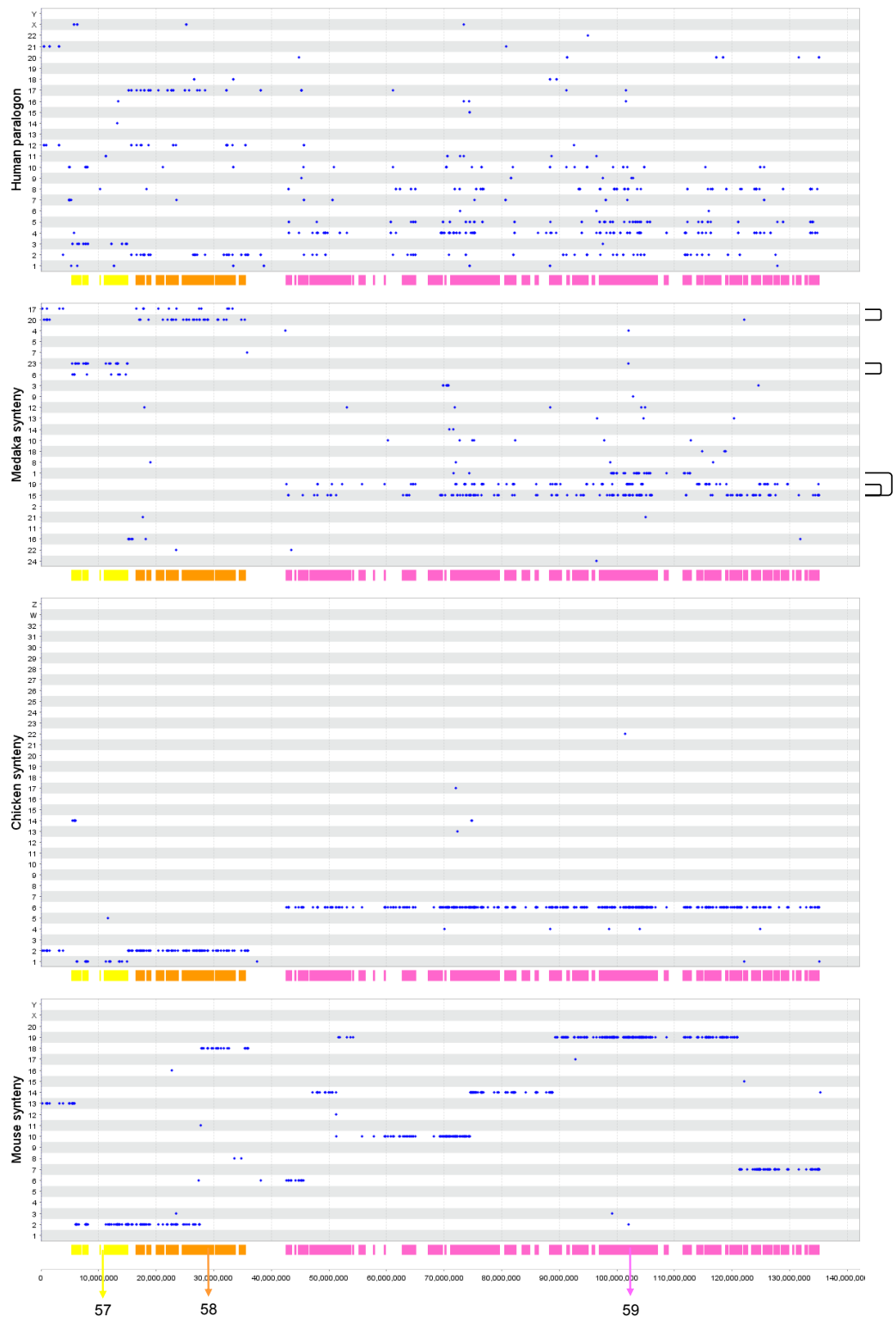


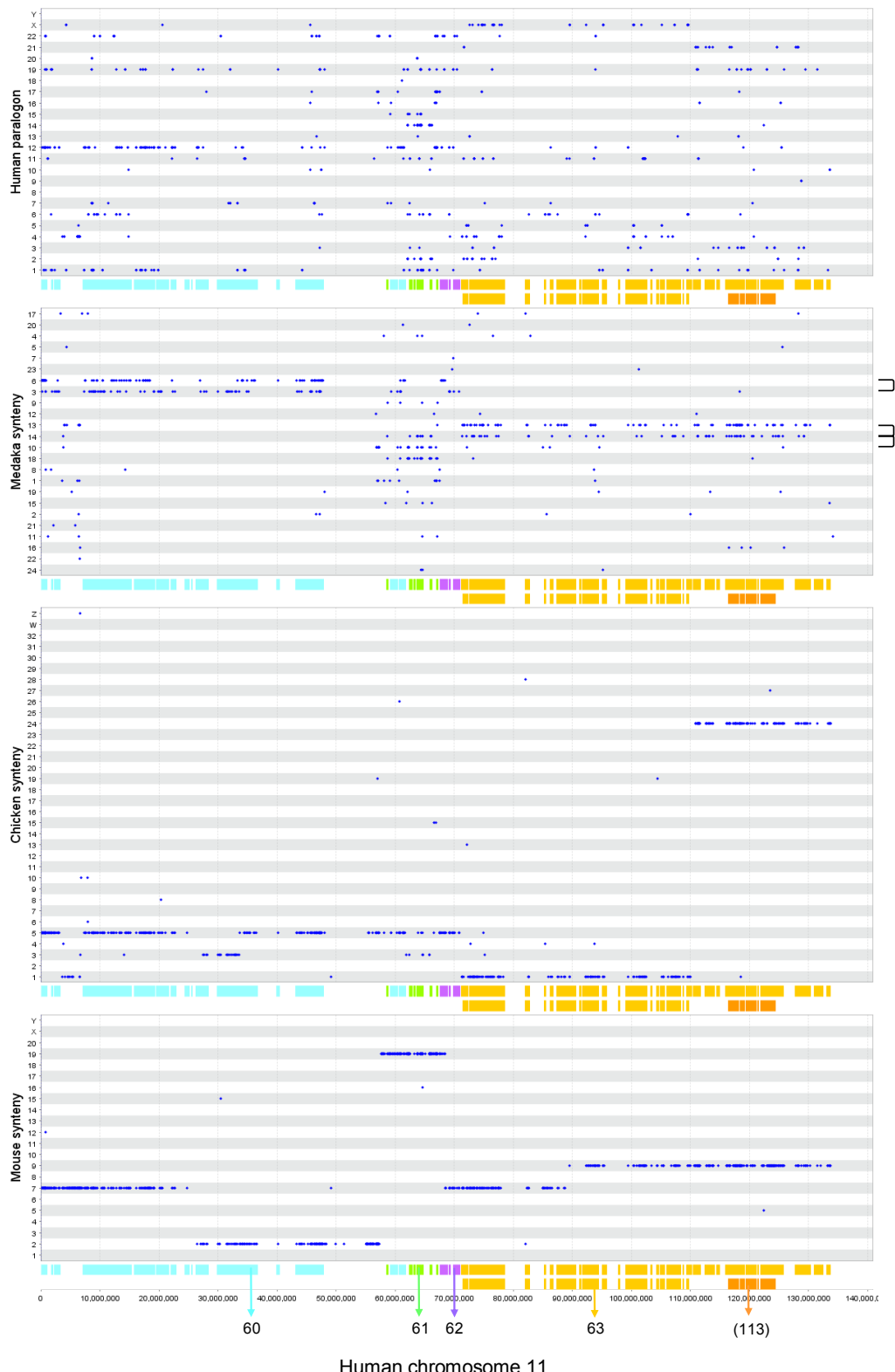


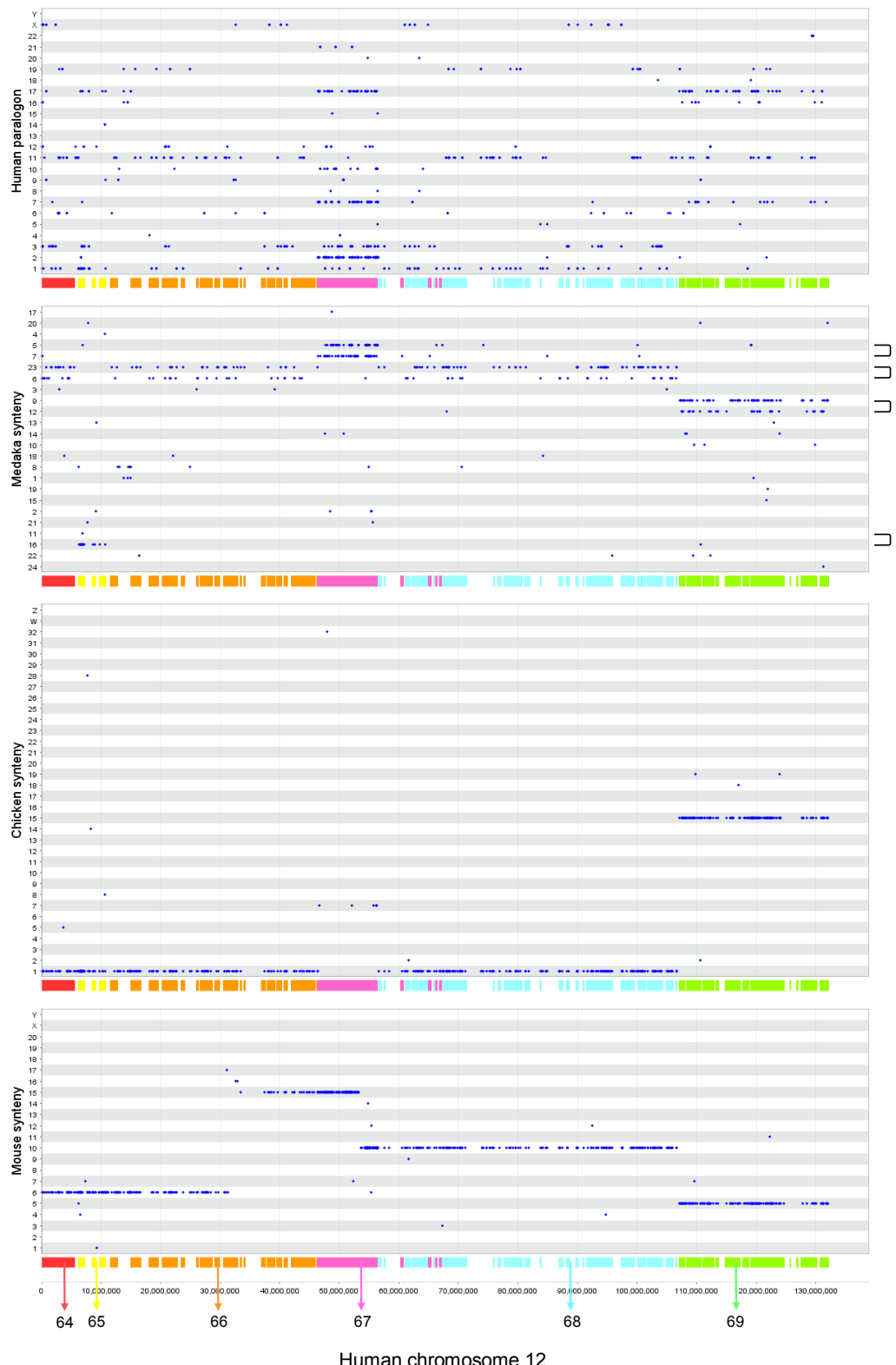


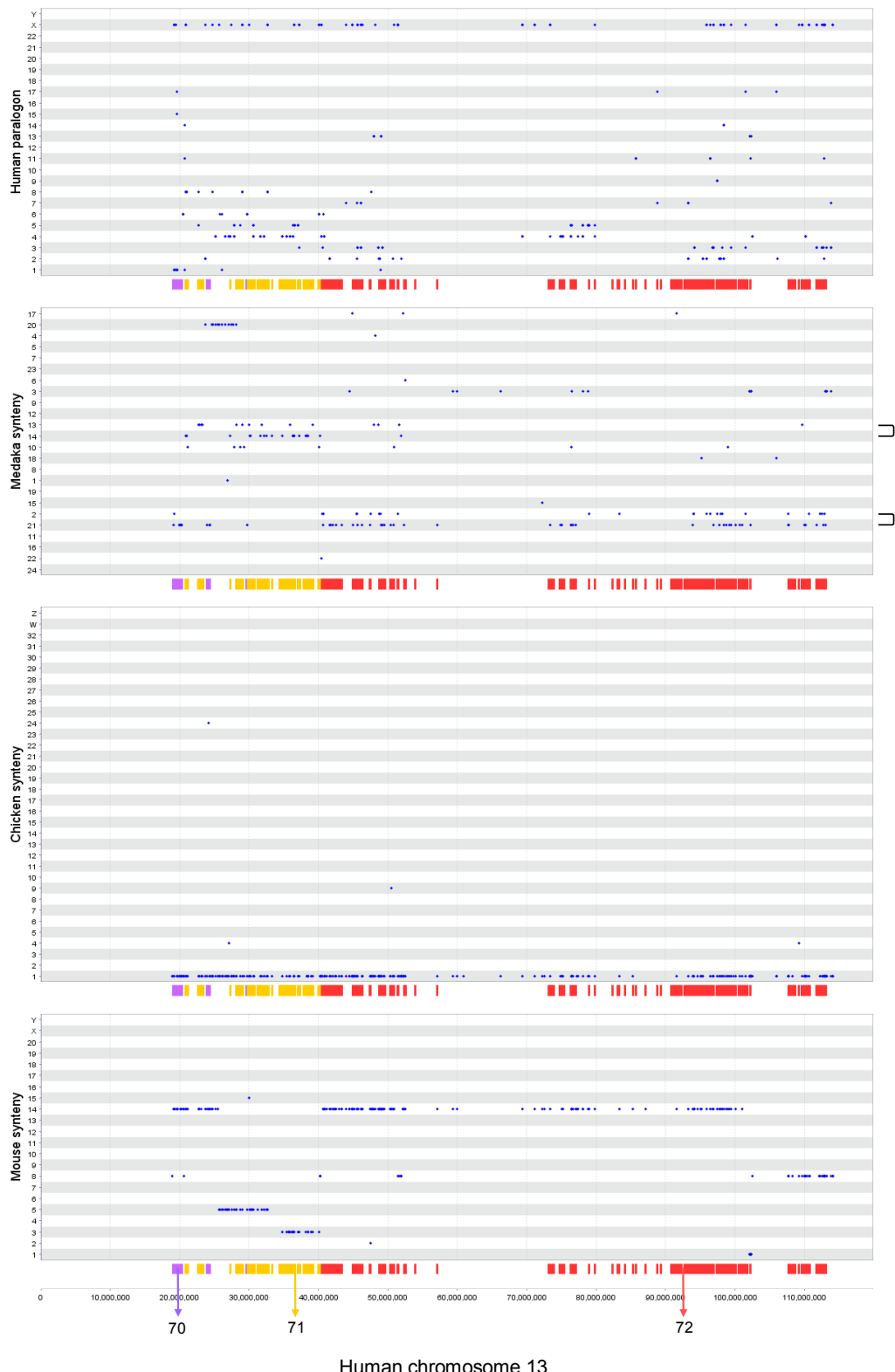


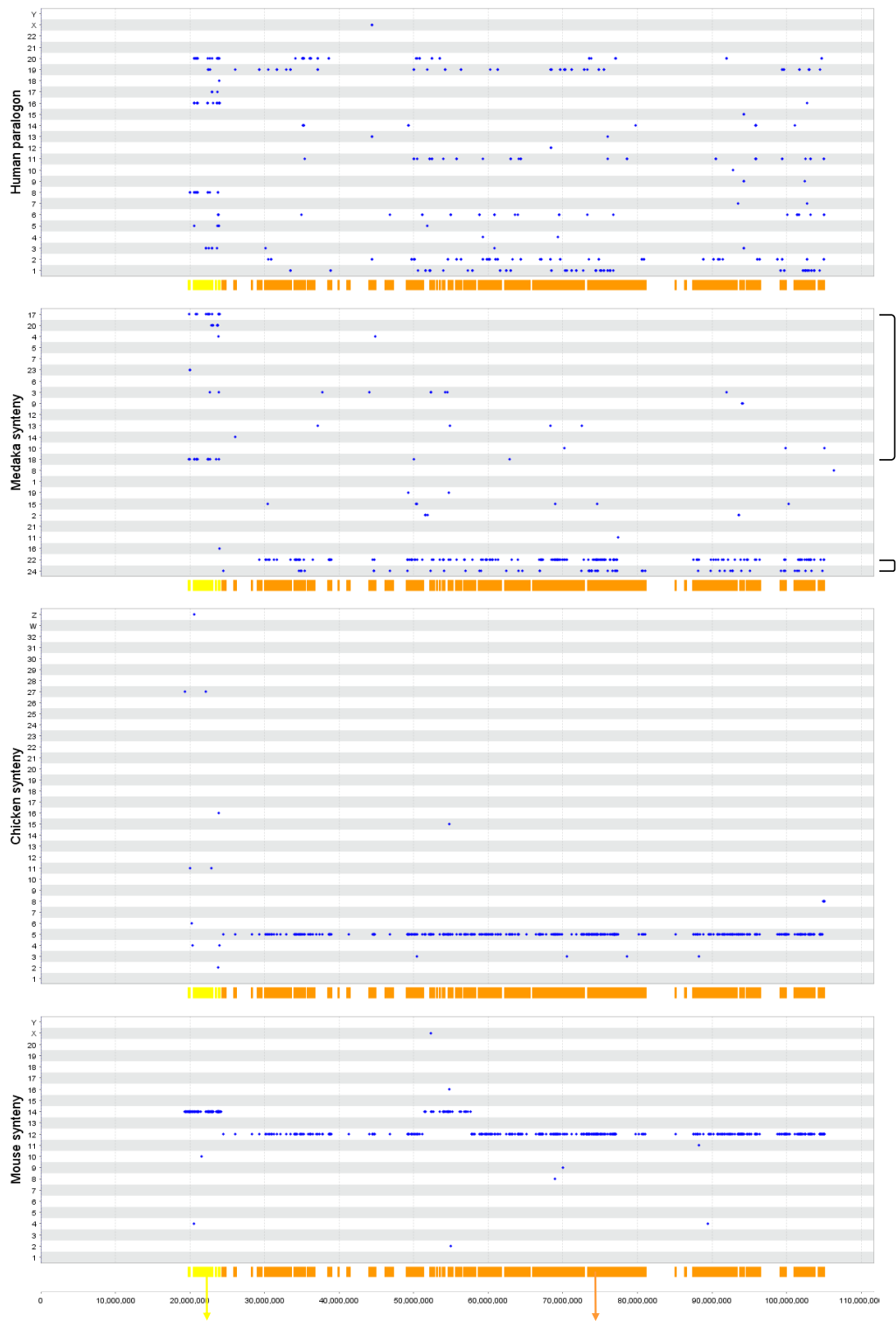


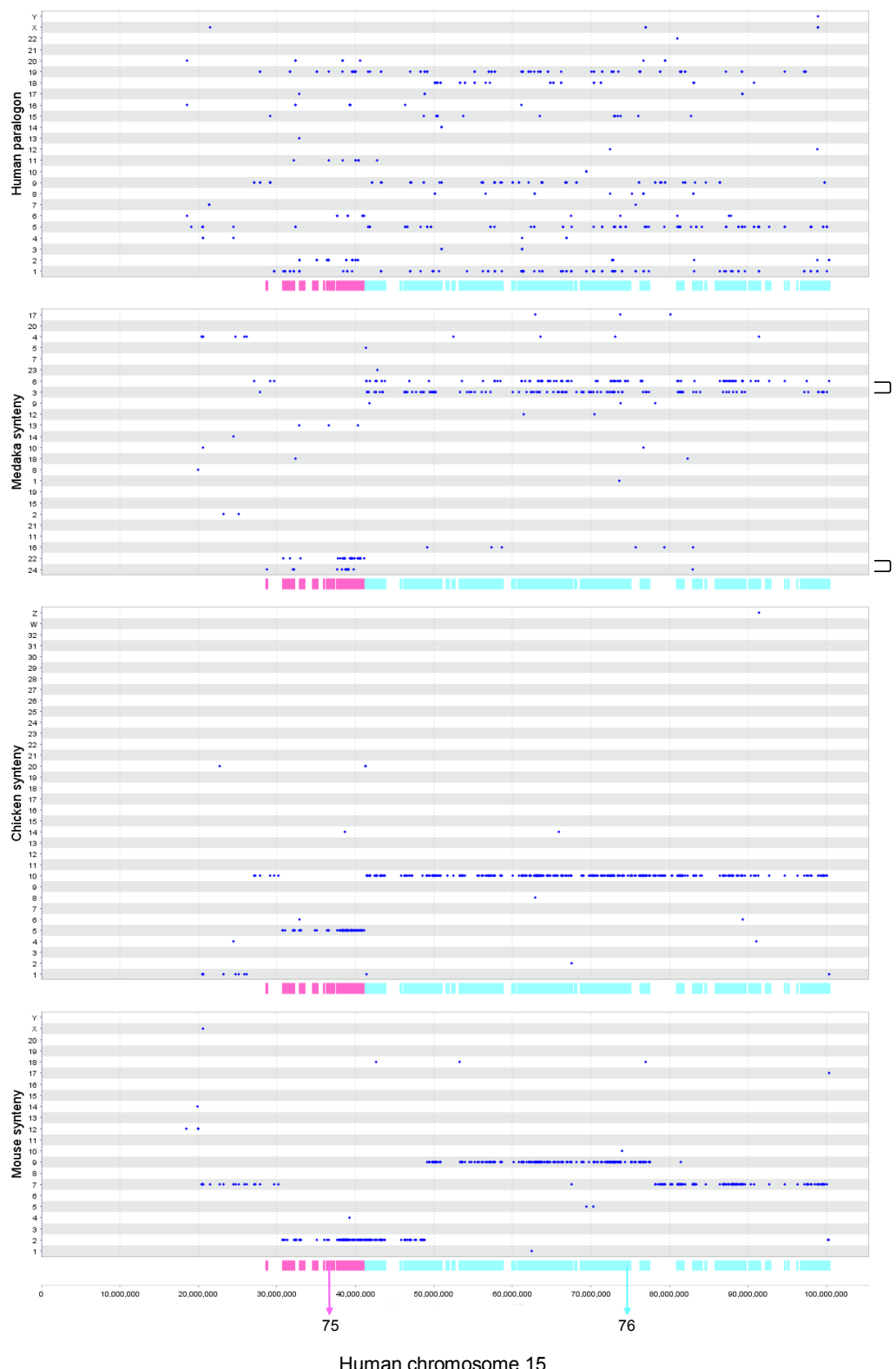


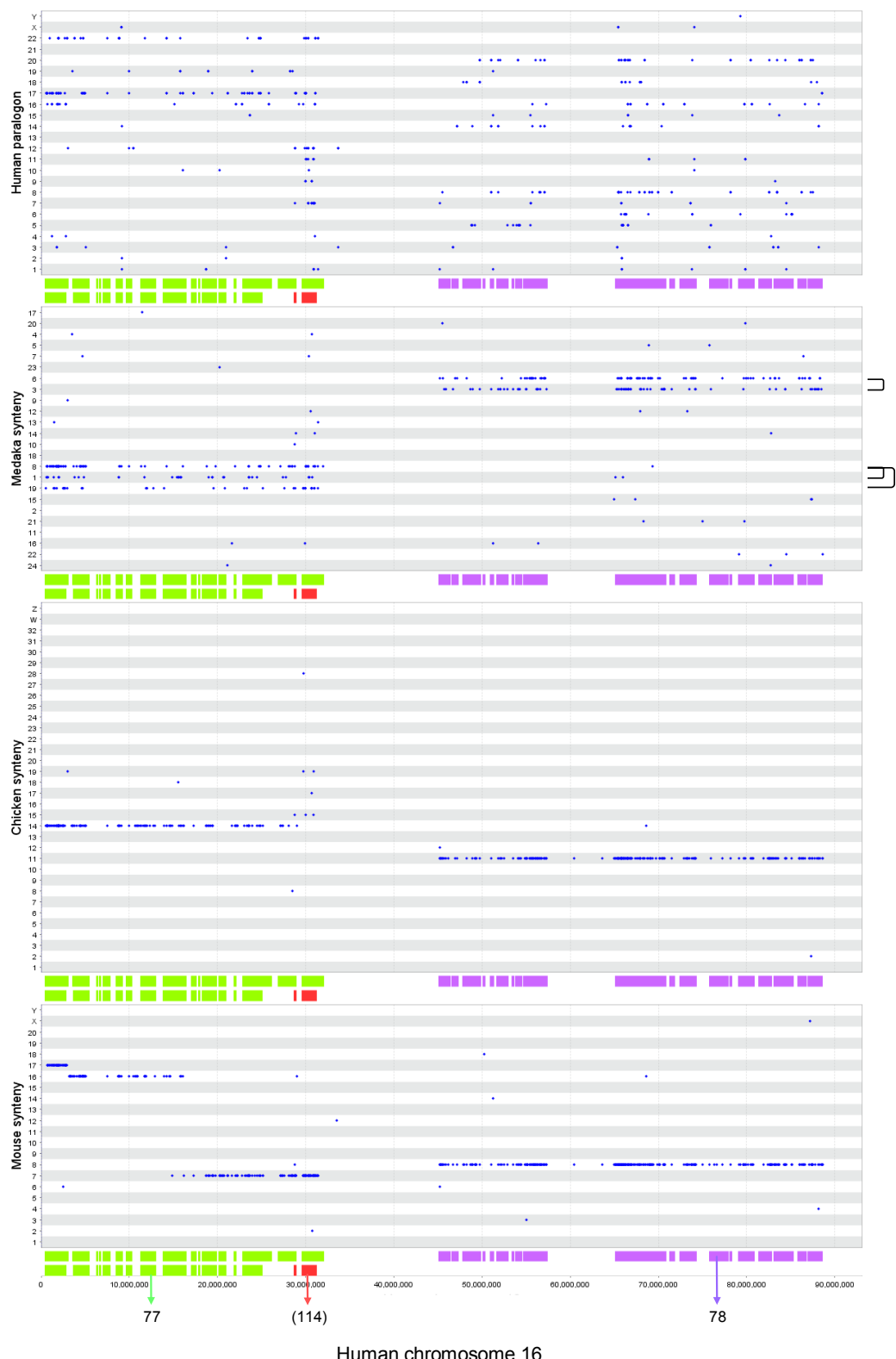


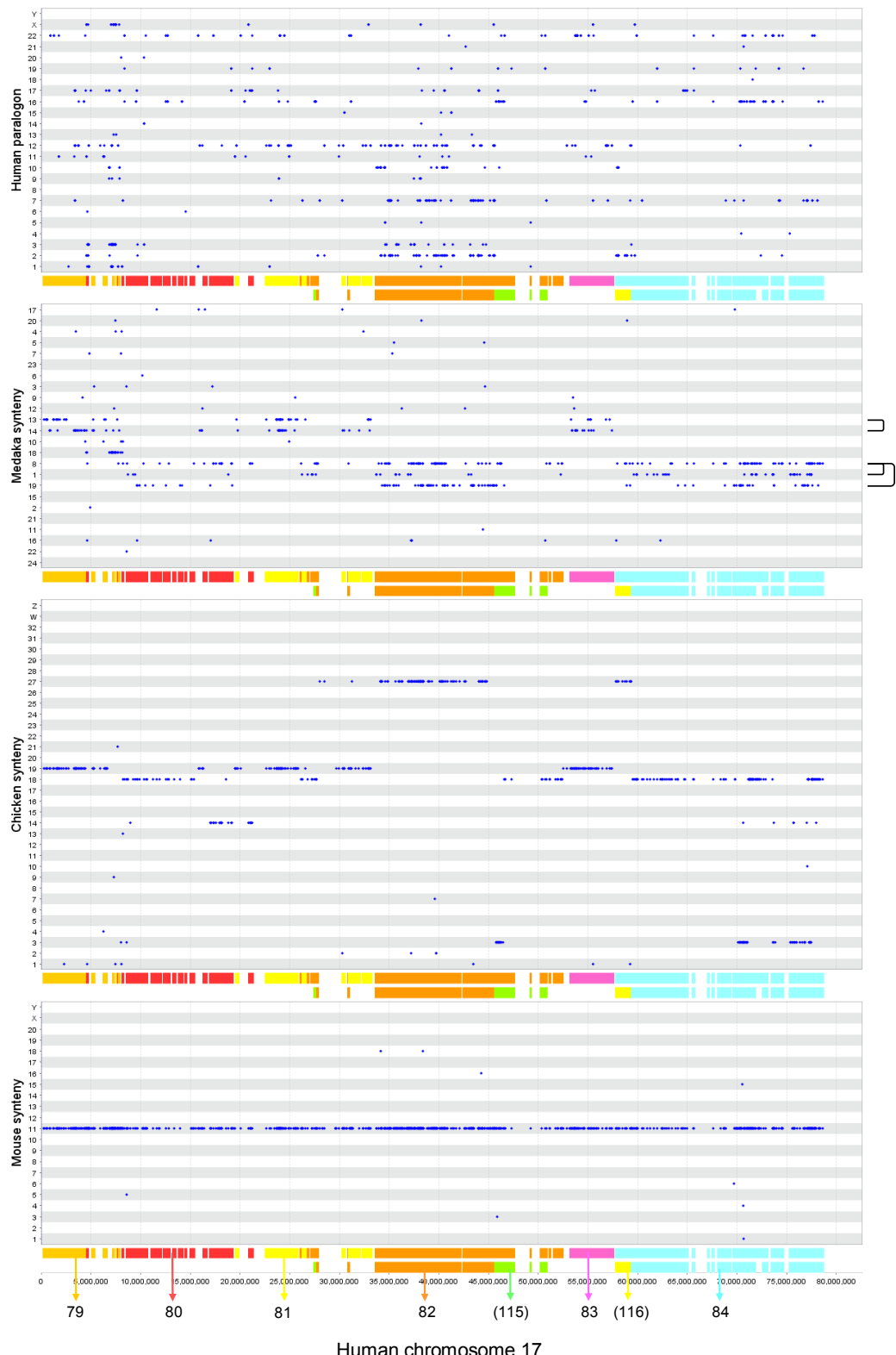


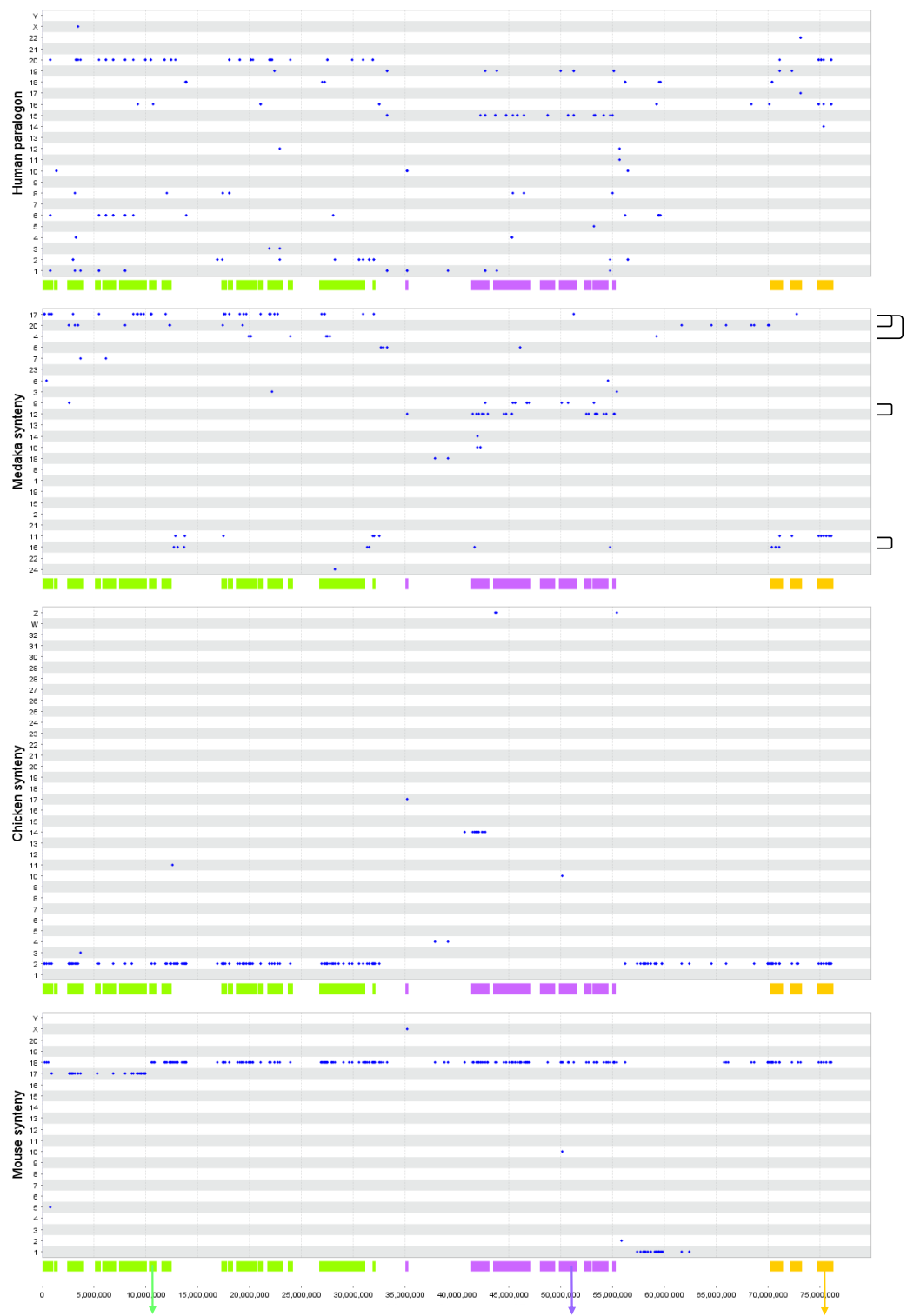


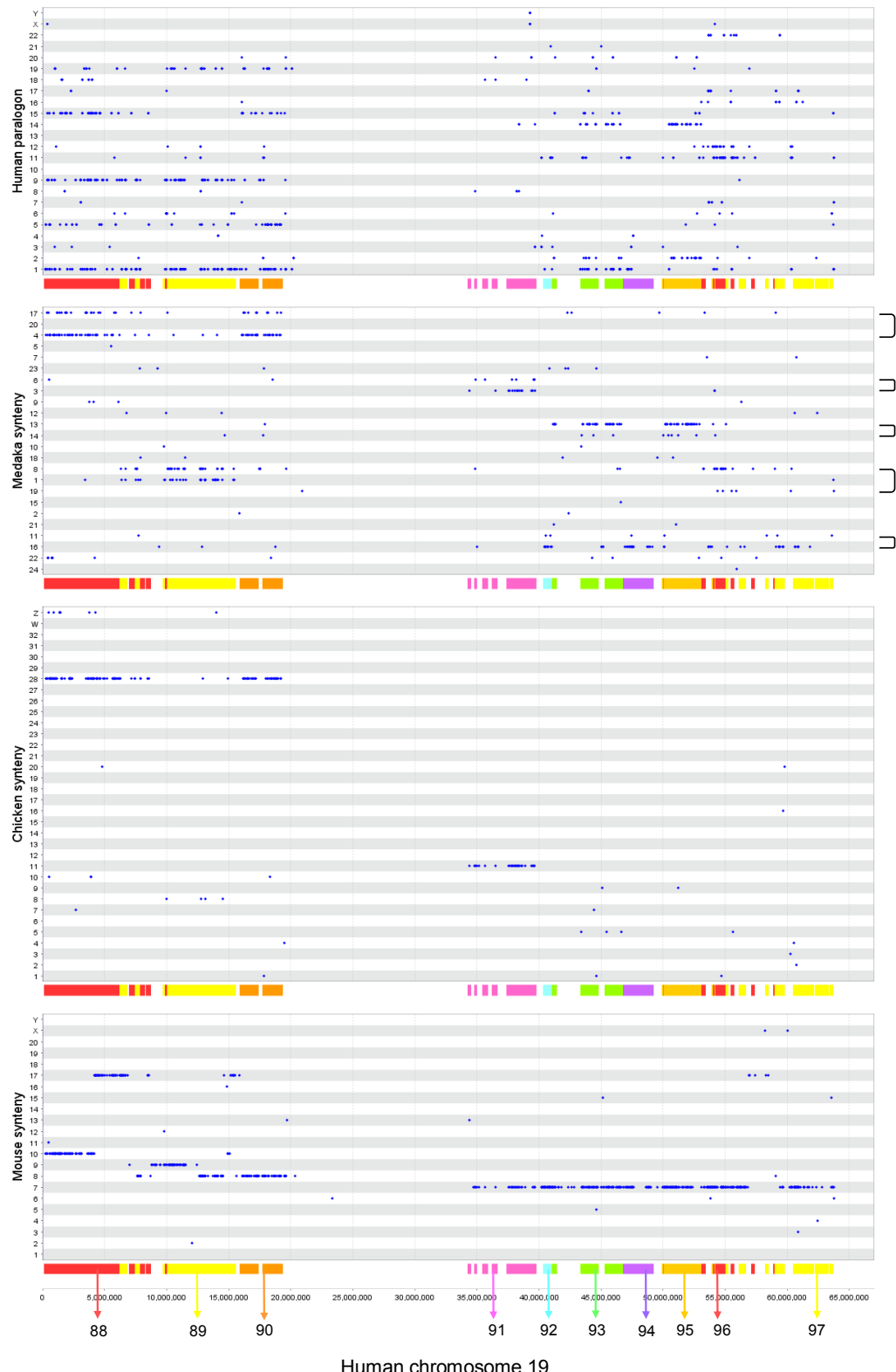


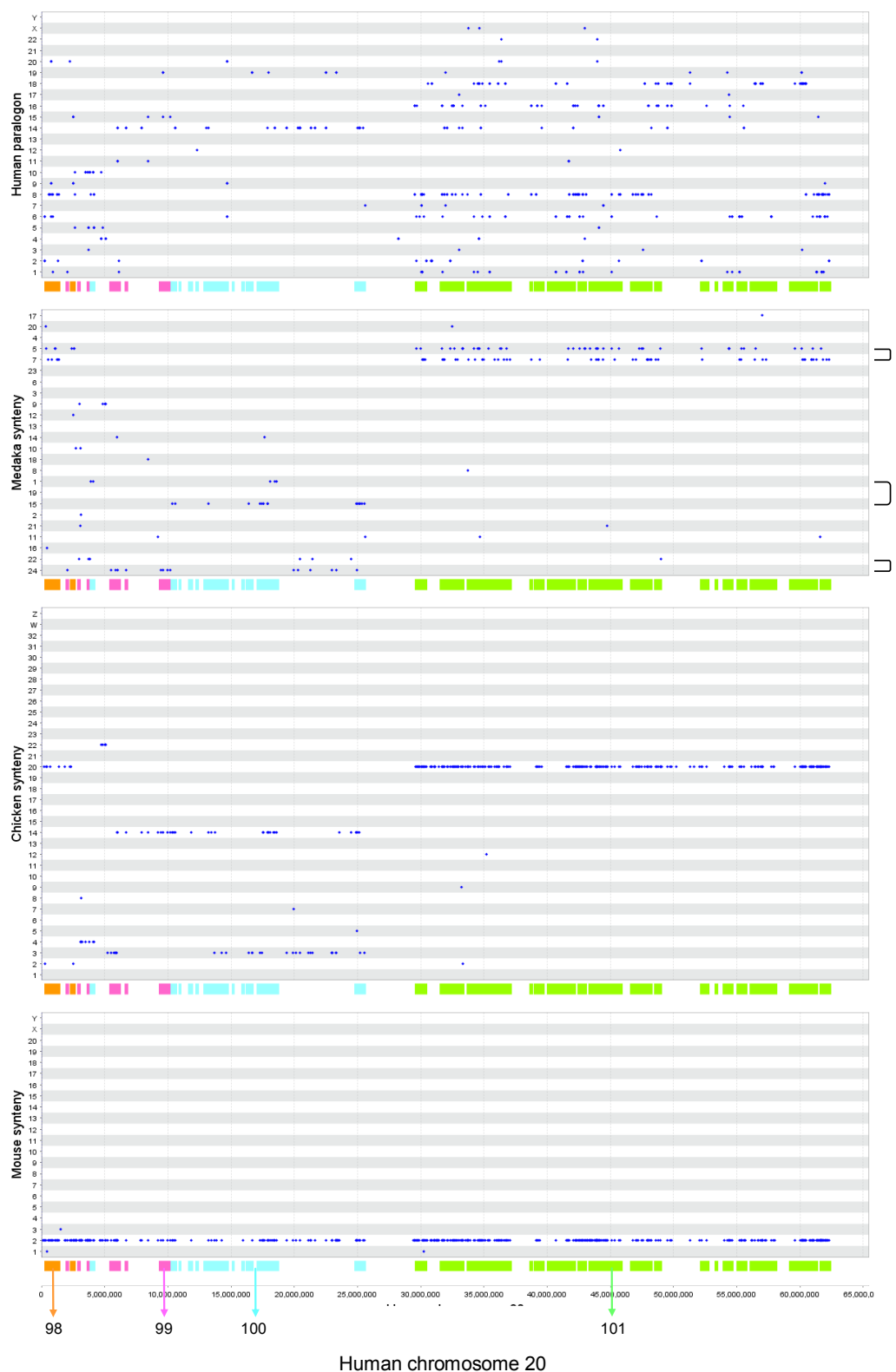






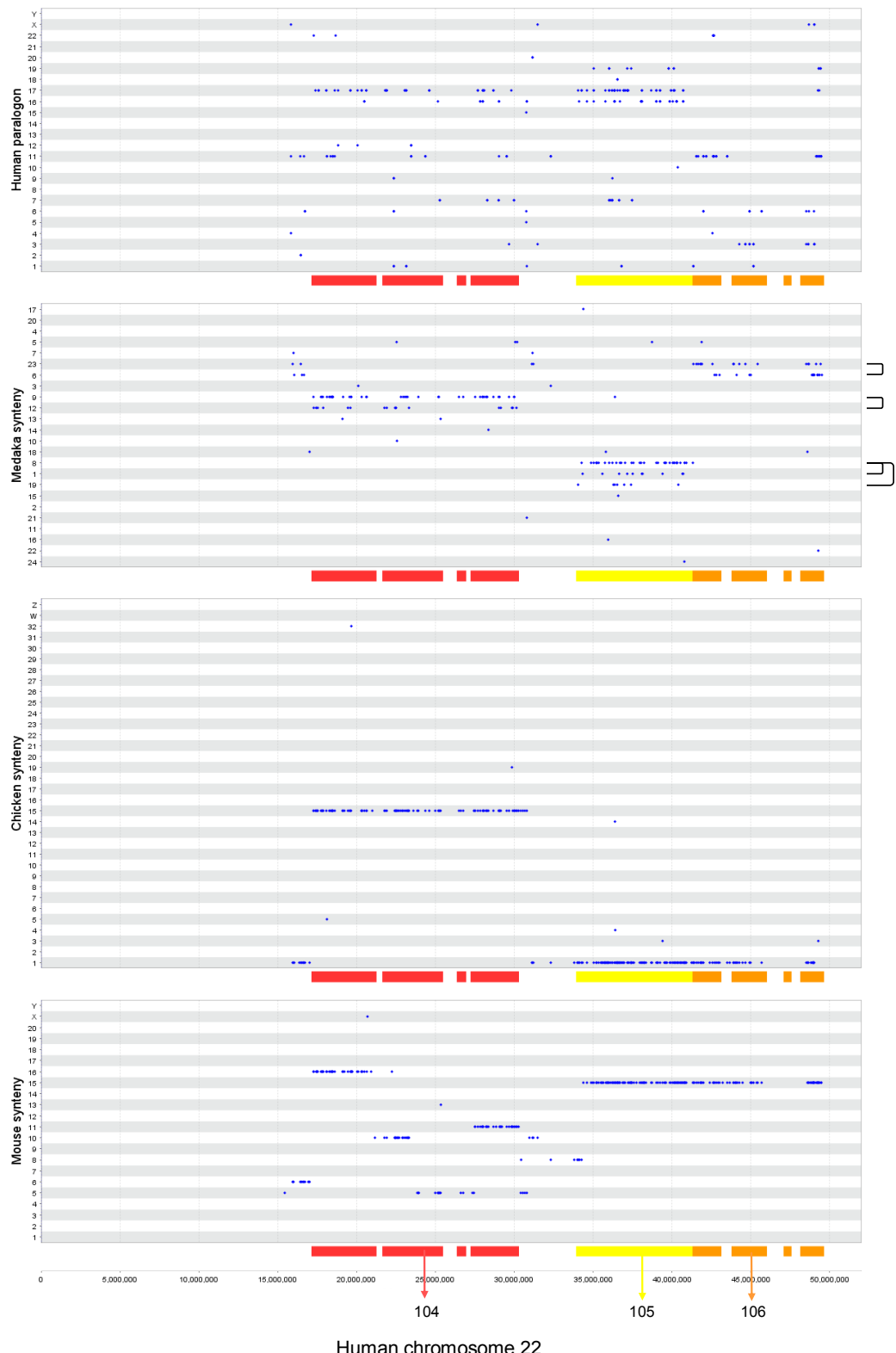




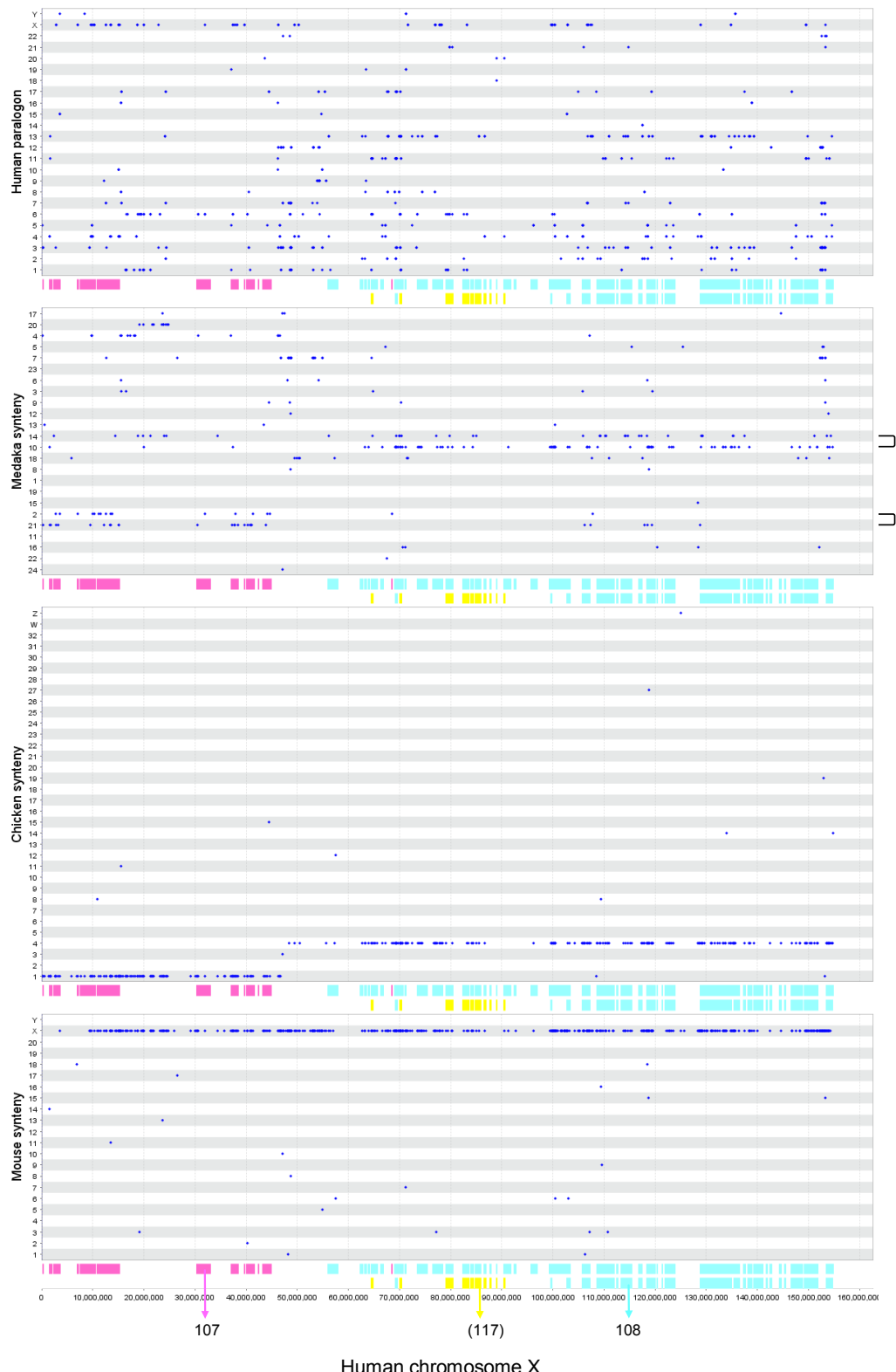


Human chromosome 20



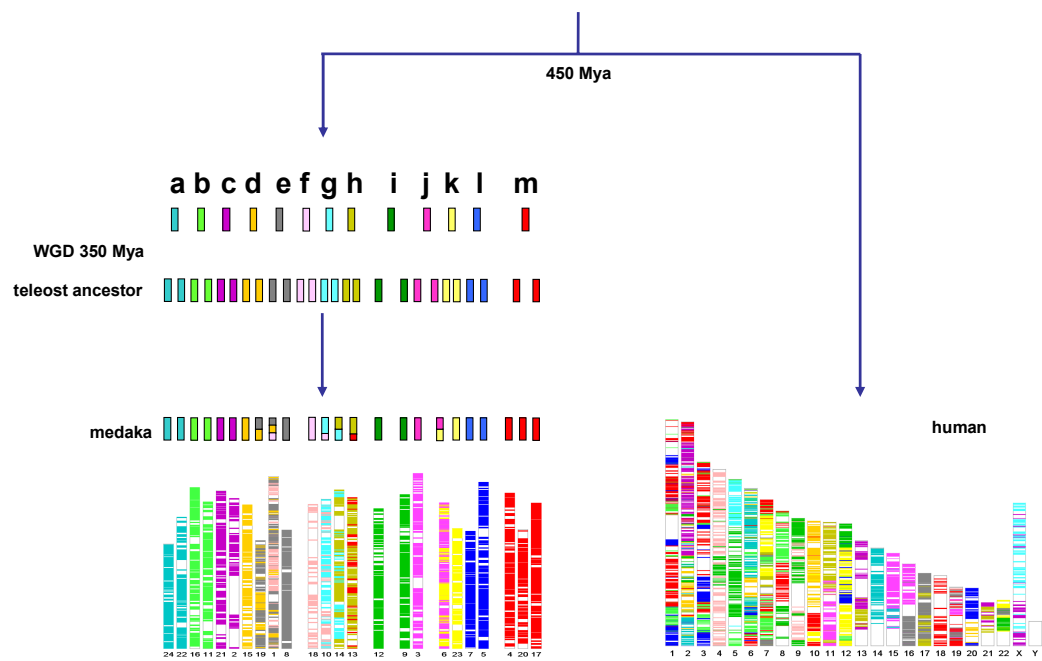


Human chromosome 22



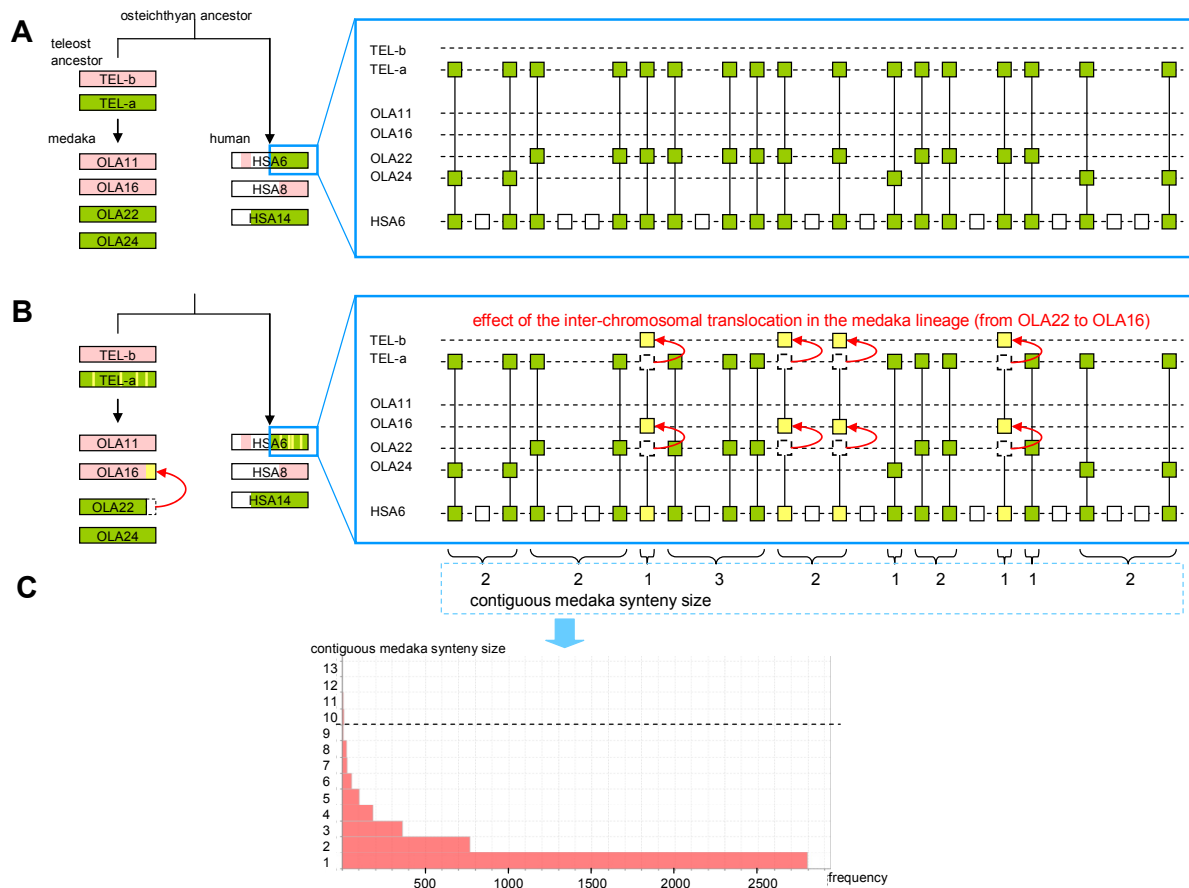


### Supplementary Figure S3



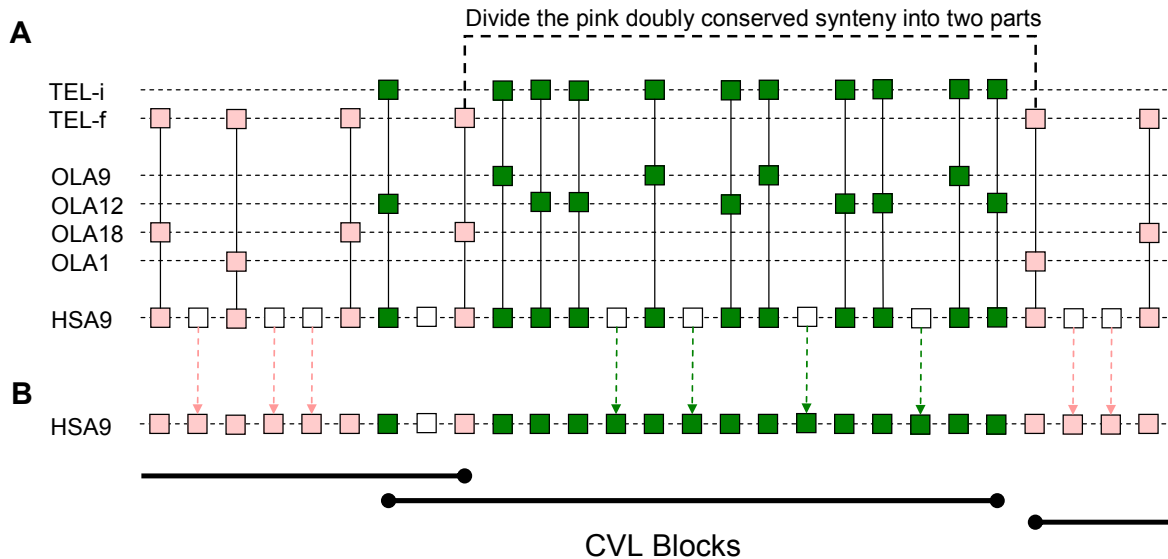
**Doubly conserved synteny (DCS) regions between the human and medaka genomes.** Thirteen proto-chromosomes before the teleost whole-genome duplication that yielded the ancestral teleost karyotype are colored differently for visualizing DCS regions between the medaka and human genomes.

### Supplementary Figure S4



**Effects of rearrangements in doubly conserved synteny (DCS) regions.** **A.** In an ideal case of CVL block construction, a translocation occurred in the human lineage. The green chromosomal region is distributed in HSA6 and HSA14, and human genes in the green region of HSA6 have medaka orthologs in OLA22 or OLA24. These genes are properly assigned to reconstructed teleost ancestor chromosome a. **B.** Effect of translocation in the medaka lineage. The four yellow genes were originally located in the teleost ancestor chromosome TEL-a, but after whole-genome duplication (WGD) were translocated from OLA22 to OLA16 in the medaka lineage. In this case, the yellow human genes have medaka orthologs in OLA16 and are erroneously assigned to TEL-b. **C.** Distribution of contiguous medaka synteny sizes. The vertical axis shows the size of contiguous human genes that have orthologs in the same medaka chromosome and are not interrupted by orthologs to different medaka chromosomes; the horizontal axis shows the frequency of the synteny size in the human genome. Contiguous medaka synteny size is very small because of the massive gene loss after WGD that occurred randomly between duplicated chromosomes.

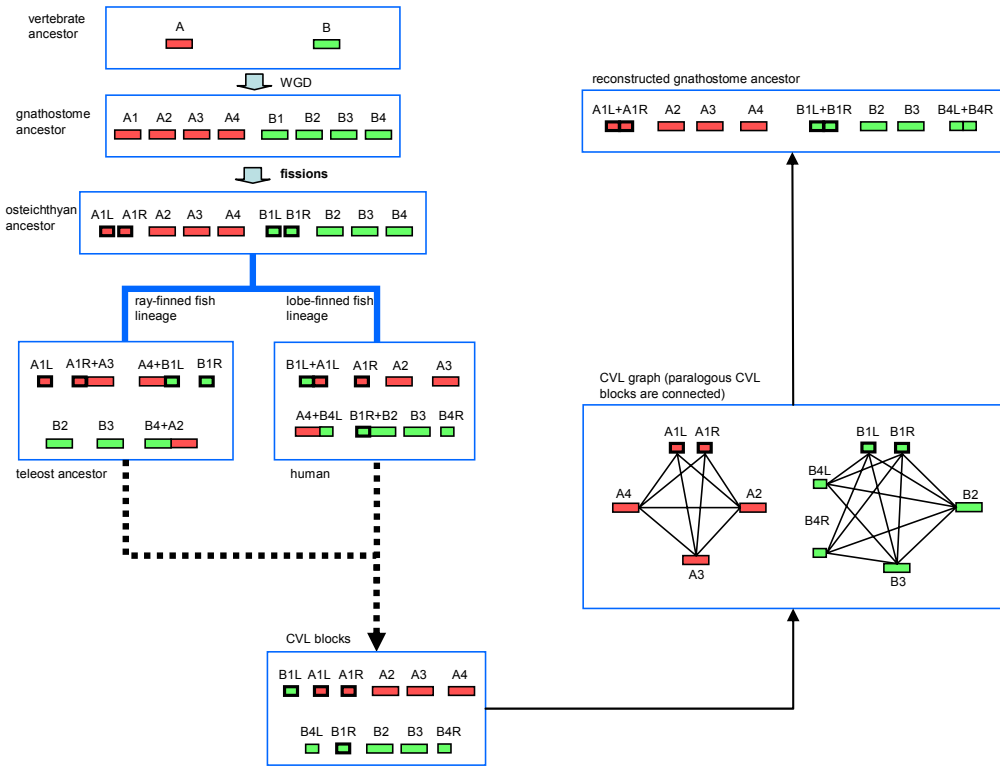
## Supplementary Figure S5



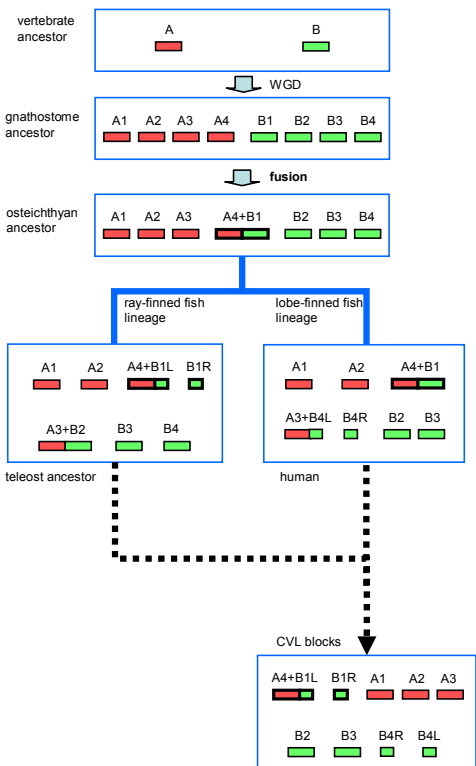
**Breaking a doubly conserved synteny (DCS) region into two blocks.** The Figure illustrates a subregion of human genes on human chromosome 9. **A.** Small boxes indicate genes; pink genes have orthologs in medaka chromosome OLA18 or OLA1 that originated from the proto-chromosome “f” in the teleost ancestor. Similarly, green genes are associated with the proto-chromosome “i” via OLA9 and OLA12. White genes have no orthologs and are not assigned to any medaka chromosome. Because 10 green genes divide the series of pink genes, they are treated as three distinct CVL blocks. **B.** After the generation of the three CVL blocks, some white genes were incorporated into the surrounding CVL blocks.

## Supplementary Figure S6

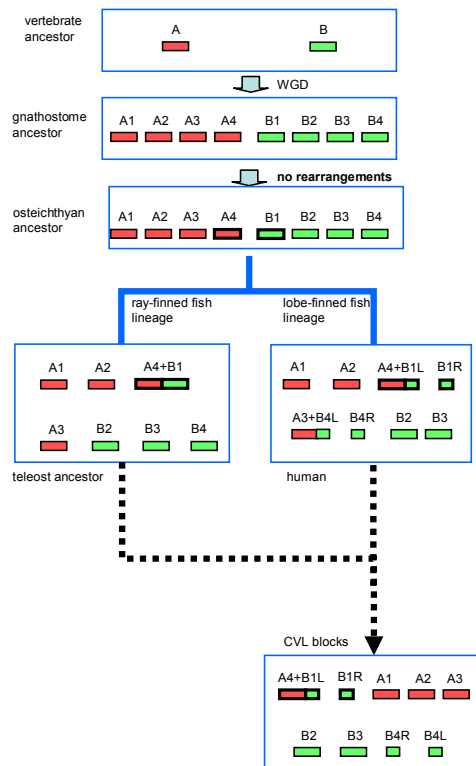
### A: effect of fissions in early vertebrate evolution

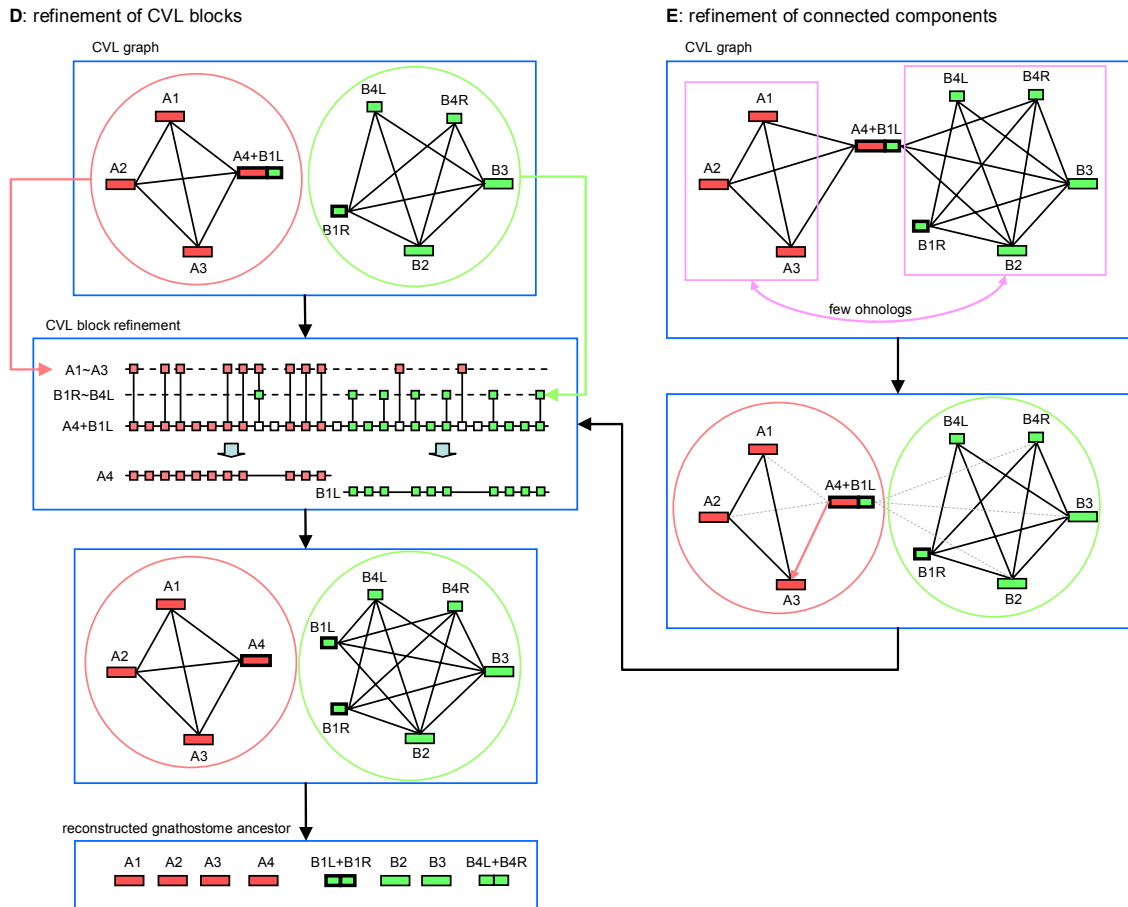


### B: effect of fusions in early vertebrate evolution



### C: effect of independent fusions in the teleost ancestor and human lineages





**Effect of ancestral rearrangements.** **A.** Chromosome fission events took place before the osteichthyan ancestor. We can reconstruct the CVL blocks by segmenting the human genome according to teleost ancestor synteny. **B.** Fusion events before the osteichthyan ancestor are likely to produce improper CVL blocks originating from multiple proto-chromosomes in the vertebrate ancestor. **C.** Similarly, erroneous CVL blocks may result from extensive rearrangements in the teleost and human lineages. **D.** Fused CVL blocks can be identified by mapping red and green ohnologs to each CVL block. **E.** Fused CVL blocks may incorrectly assign CVL blocks derived from two vertebrate proto-chromosomes to one connected component. This error can be fixed by checking the number of ohnologs between two subcomponents.

## Supplementary Figure S7

**Reconstruction of proto-chromosomes using CVL blocks.** Ten reconstructed proto-chromosomes, A–J, are displayed. **A.** The most significant five candidates of the duplicated sister chromosomes in each proto-chromosome. The first column shows the significance of each candidate, and the remaining columns present groups of CVL blocks that constitute sister chromosomes. **B.** The table shows how genes in the vertebrate proto-chromosome are distributed in the human, teleost ancestor, and chicken genomes. The first two columns present the identifiers of CVL blocks, and the number of genes in the CVL block. The next three columns display the syntenic chromosomes in the human, teleost ancestor, and chicken genomes. The remaining columns present the numbers of orthologs shared between the CVL blocks and individual chicken chromosomes. **C.** For the most significant reconstruction of sister chromosomes, dots are plotted for ohnologs in the matrix of CVL blocks grouped by sister chromosomes. **D.** The figure presents another representation of ohnologs in which CVL blocks are placed on a circle, and curved lines indicate ohnologs between CVL blocks. **E.** The strength of the correlation between CVL blocks in terms of ohnologs is visualized using a graph in which each node represents a CVL block labeled with its identifier, its human chromosome number, its teleost proto-chromosome number, and its size. The connected lines between CVL block nodes represent the significance of the number of shared ohnologs. Bold lines indicate significant relations with the probability  $<0.0001$ , while dotted lines indicate the probability  $<0.001$ .

A

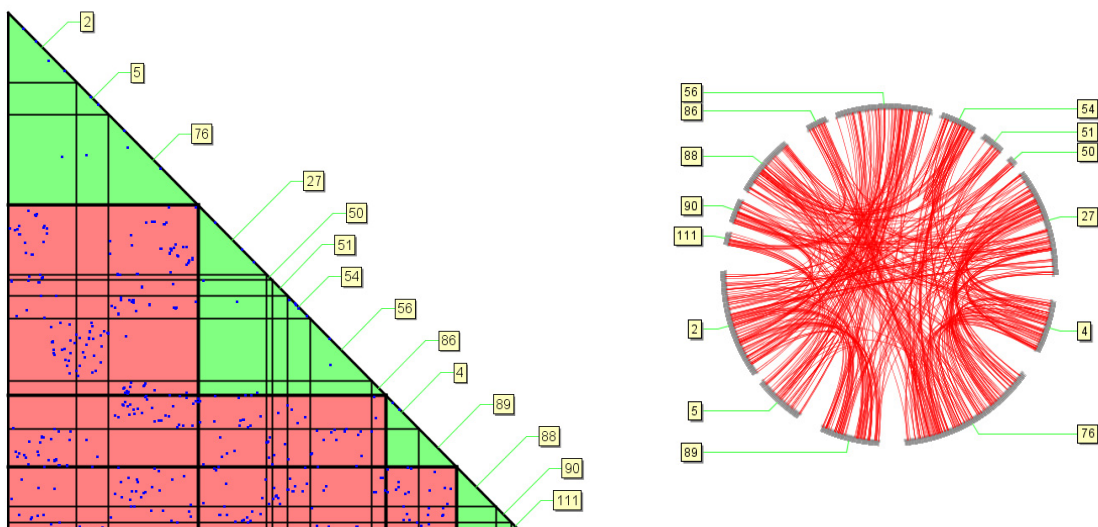
a

significance	gnathostome subgroup 1	gnathostome subgroup 2	gnathostome subgroup 3	gnathostome subgroup 4	gnathostome subgroup 5
2.72E-37	2,5,76	27,50,51,54,56,86	4,89	88,90,111	
1.42E-36	2,5,76	27,50,51,54,56,86	4,89	88,90	111
4.32E-36	2,5,76	27,50,51,54,56,86	4,89	88,111	90
8.88E-36	2,5,76	27,50,51,54,56,86	4,89	88	90,111
1.17E-35	2,5,76	27,51,54,56,86	4,89	88,90,111	50

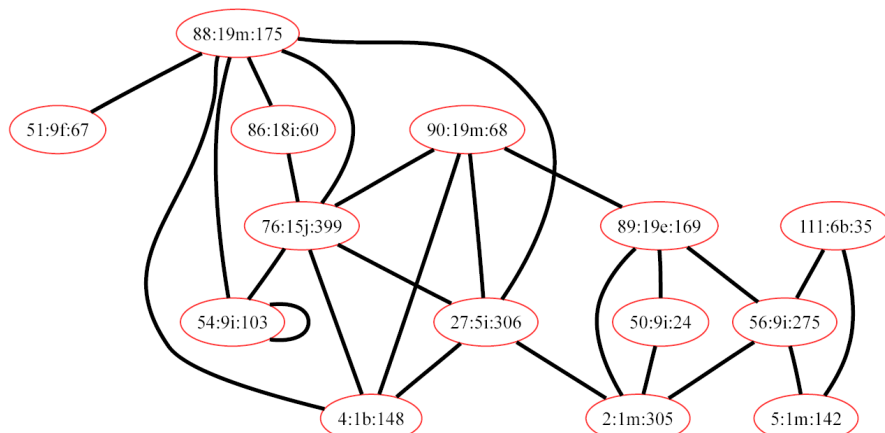
b

C

d



e



B

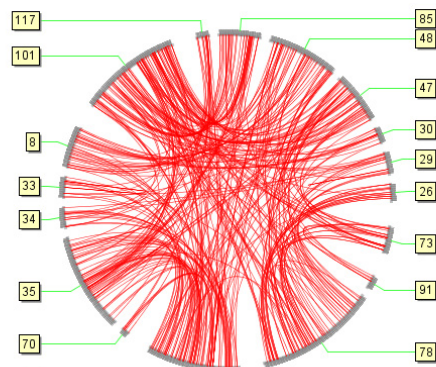
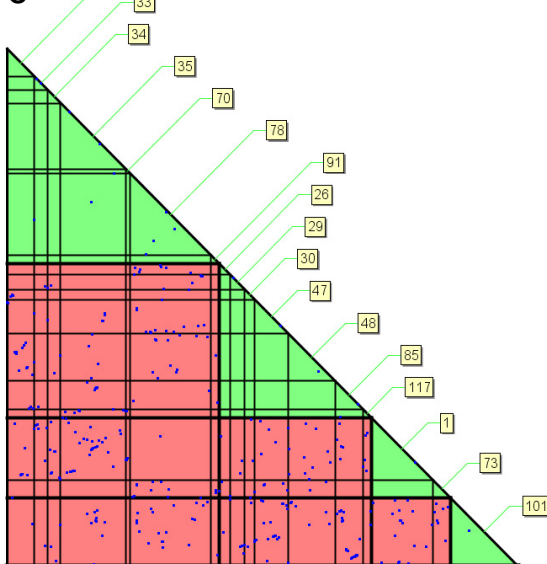
a

significance	gnathostome subgroup 1	gnathostome subgroup 2	gnathostome subgroup 3	gnathostome subgroup 4	gnathostome subgroup 5
4.62E-30	8,33,34,35,70,78,91	26,29,30,47,48,85,117	1,73	101	
4.92E-30	8,33,34,35,78,91	26,29,30,47,48,85,117	1,73	70,101	
9.02E-30	8,33,34,35,78,91	26,29,30,47,48,70,85	1,73	101	117
1.31E-29	8,33,34,35,78,91	26,29,30,47,48,85,117	1,73	101	70
2.60E-29	8,33,34,35,70,78,91	26,29,30,47,48,85	1,73	101	117

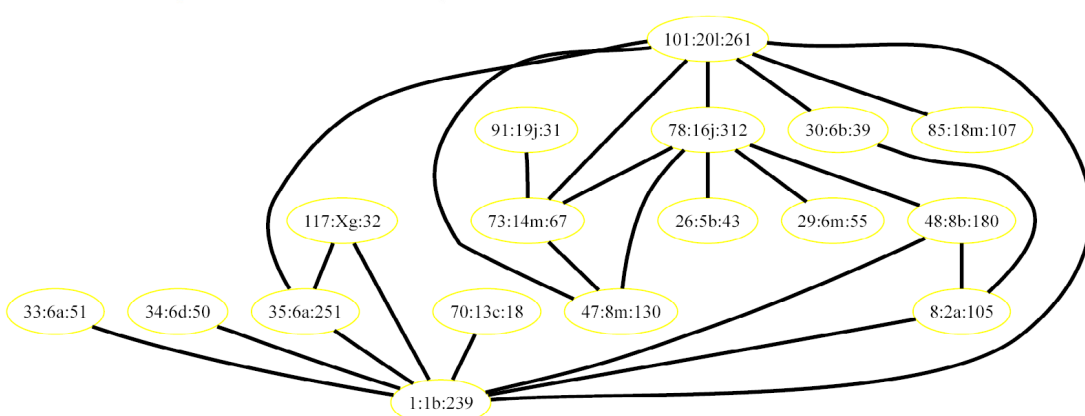
b

6

d



e



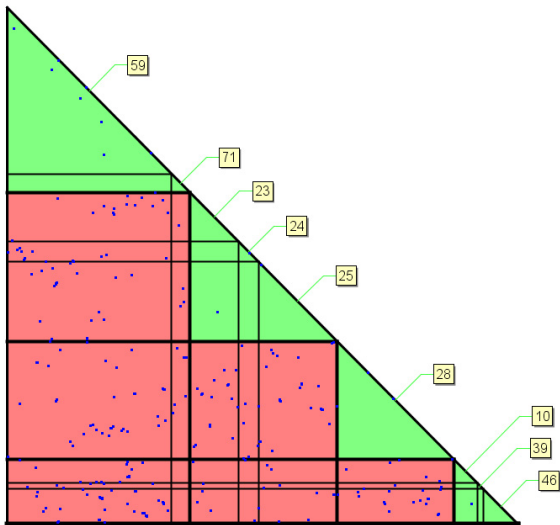
C

a

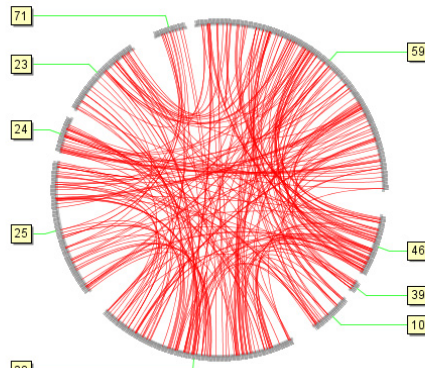
significance	gnathostome subgroup 1	gnathostome subgroup 2	gnathostome subgroup 3	gnathostome subgroup 4	gnathostome subgroup 5
9.35E-20	59,71	23,24,25	28	10,39,46	
1.14E-19	59,71	23,24,25	28	39,46	10
1.32E-19	59,71	23,24,25	28	46	10,39
1.97E-19	59,71	23,24,25	28	10,46	39
5.30E-19	59,71	10,23,24,25	28	39,46	

b

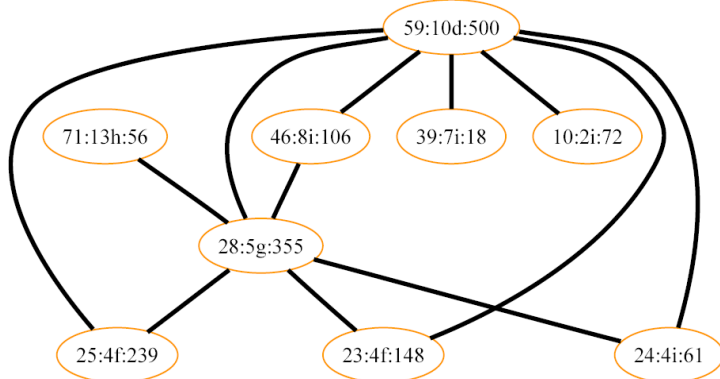
C



d



e



D

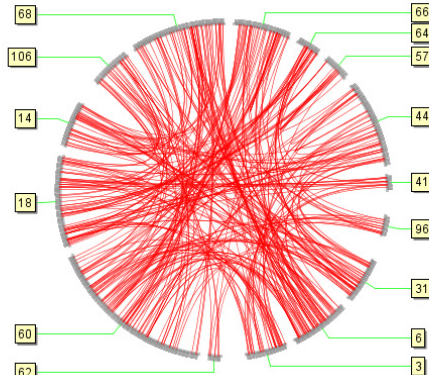
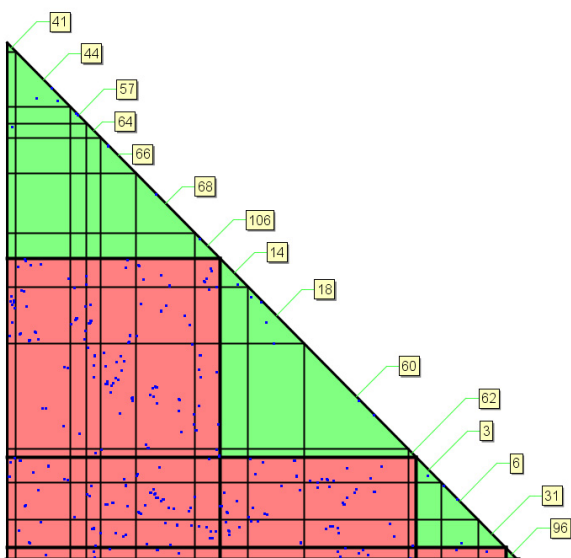
a

significance	gnathostome subgroup 1	gnathostome subgroup 2	gnathostome subgroup 3	gnathostome subgroup 4	gnathostome subgroup 5
2.36E-30	41,44,57,64,66,68,106	14,18,60,62	3,6,31	96	
4.52E-30	41,44,57,64,66,68,106	14,18,60,62	3,6,31,96		
3.61E-29	41,44,57,64,66,68,106	14,18,60,62	3,6,96	31	
4.47E-29	44,57,64,66,68,106	14,18,60,62	3,6,31	41,96	
4.53E-29	41,44,57,64,66,68,106	14,18,60,62	3,6	31	96

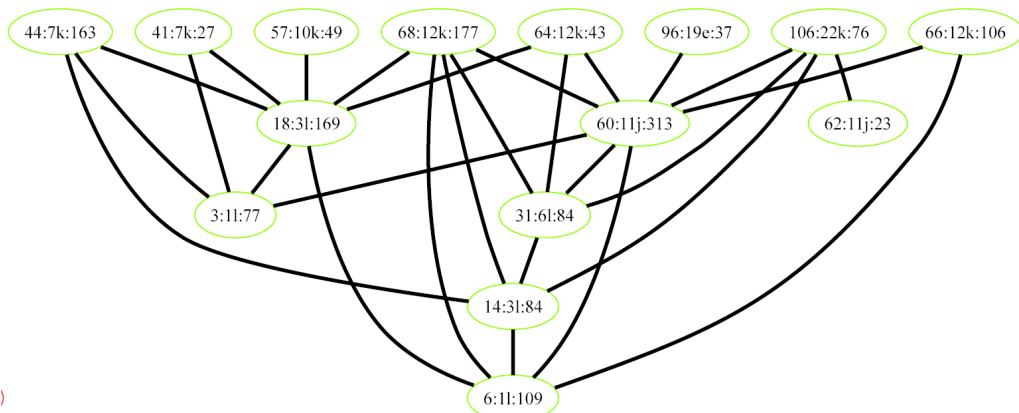
b

C

d



e



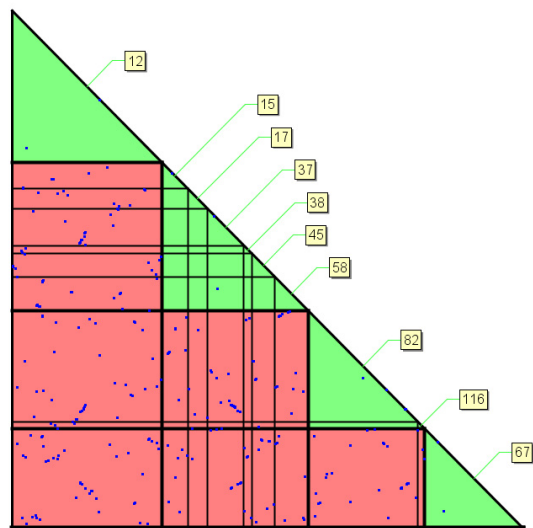
E

a

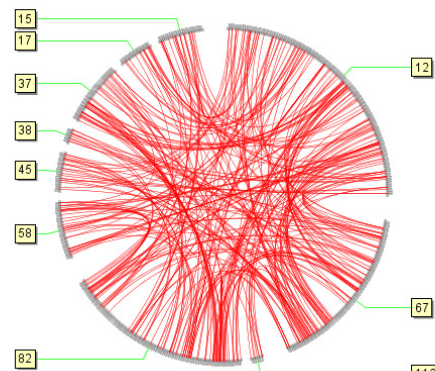
significance	gnathostome subgroup 1	gnathostome subgroup 2	gnathostome subgroup 3	gnathostome subgroup 4	gnathostome subgroup 5
4.00E-20	12	15,17,37,38,45,58	82,116	67	
2.21E-19	12	15,17,37,38,45,58	82	67	116
4.99E-19	12	15,17,37,45,58	82,116	67	38
9.48E-19	12	15,37,38,45,58	17,67	82,116	
9.94E-19	15,17,37,38,45,58,116	12	82	67	

b

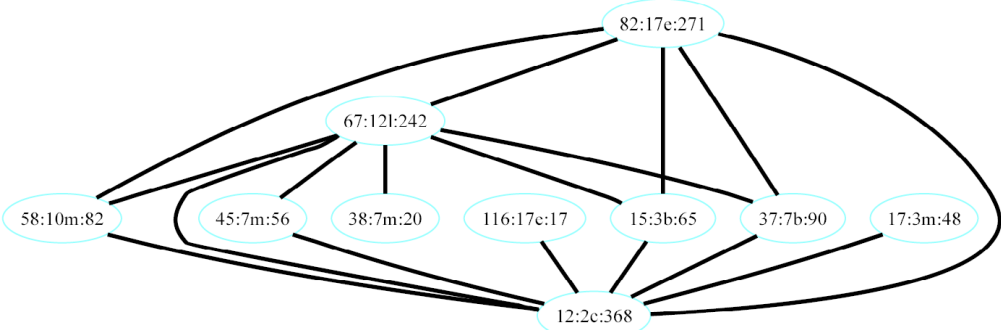
C



d



e



F

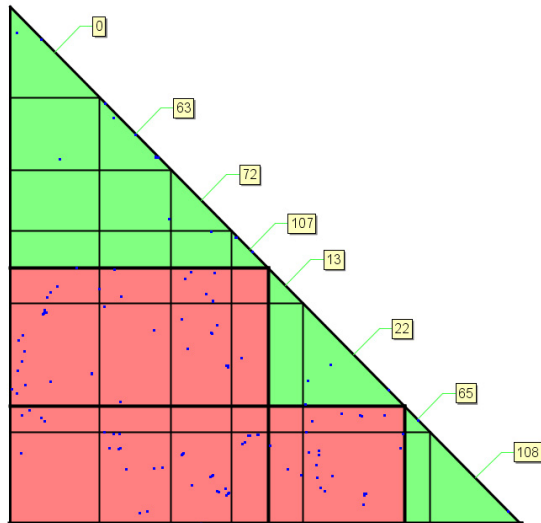
a

significance	gnathostome subgroup 1	gnathostome subgroup 2	gnathostome subgroup 3	gnathostome subgroup 4	gnathostome subgroup 5
1.02E-06	0,63,72,107	13,22	65,108		
1.83E-06	0,63,65,72,107	13,22	108		
6.43E-06	0,63,72,107	13,22	108	65	
1.19E-05	0,63,72	13,22,107	65,108		
1.30E-05	0,63,72,107	13,65,108	22		

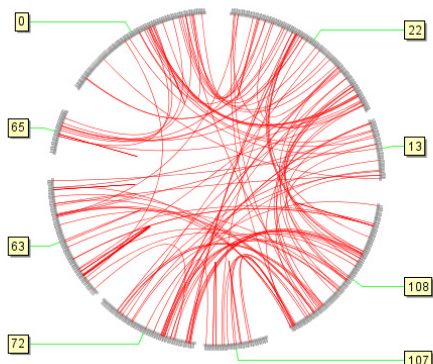
b

ID	gene	human	teleost	chicken	1	2	3	4	5	6	7	8	9	10	11	12	13	14	15	16	17	18	19	20	21	22	23	24	25	26	27	28	29	30	31	32	W	Z	Un
0	215	1	I	21,Un	0	0	0	0	0	0	0	0	0	0	0	0	0	0	0	0	0	0	0	0	0	0	0	0	0	0	0	0	0	0	0	0	0	4	
63	173	11	h	1	92	0	0	0	0	0	0	0	0	0	0	0	0	0	0	0	0	0	0	0	0	0	0	0	0	0	0	0	0	0	0	0	0		
72	144	13	c	1	86	0	0	0	0	0	0	0	0	0	0	0	0	0	0	0	0	0	0	0	0	0	0	0	0	0	0	0	0	0	0	0			
107	89	X	c	1	56	0	0	0	0	0	0	0	0	0	0	0	0	0	0	0	0	0	0	0	0	0	0	0	0	0	0	0	0	0	0	0			
13	83	2	m	9	0	0	0	0	0	0	0	0	0	0	0	0	0	0	0	0	0	0	0	0	0	0	0	0	0	0	0	0	0	0	0	0			
22	246	3	m	2,9	0	6	0	0	0	0	0	0	0	0	0	0	0	0	0	0	0	0	0	0	0	0	0	0	0	0	0	0	0	0	0	0			
65	61	12	b	1	26	0	0	0	0	0	0	0	0	0	0	0	0	0	0	0	0	0	0	0	0	0	0	0	0	0	0	0	0	0	0	0	0		
108	219	X	g	4	0	0	0	64	0	0	0	0	0	0	0	0	0	0	0	0	0	0	0	0	0	0	0	0	0	0	0	0	0	0	0	0	0	0	

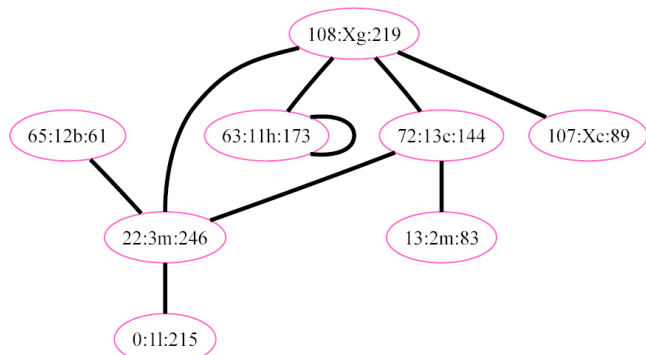
c



d



e



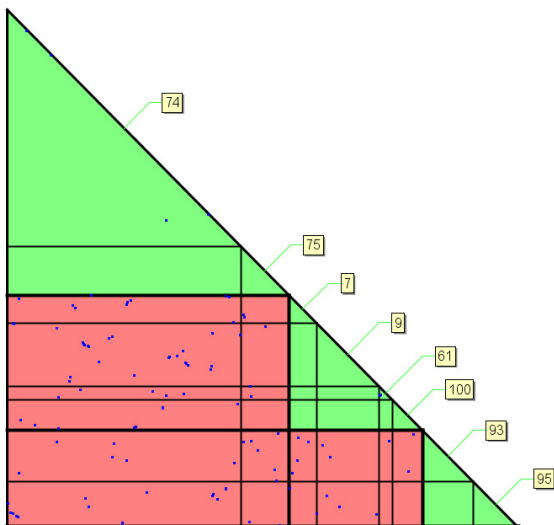
G

a

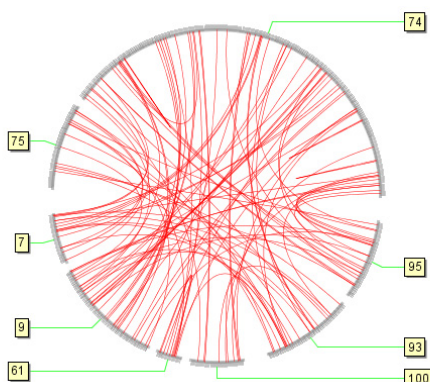
significance	gnathostome subgroup 1	gnathostome subgroup 2	gnathostome subgroup 3	gnathostome subgroup 4	gnathostome subgroup 5
1.12E-15	74.75	7,9,61,100	93.95		
7.01E-15	74.75	7,9,100	93.95	61	
1.40E-14	74.75	7,9,61,100	93	95	
1.54E-14	74.75	7,9,100	61,93,95		
2.79E-14	74.75	9,61,100	93.95	7	

b

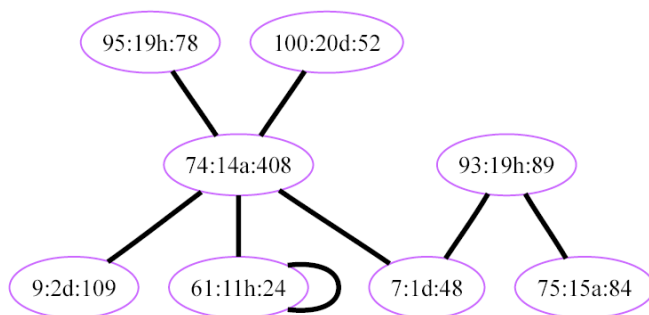
C



d



e



H

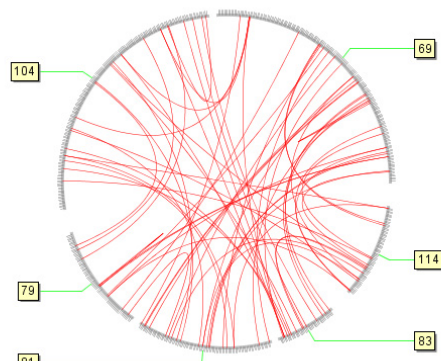
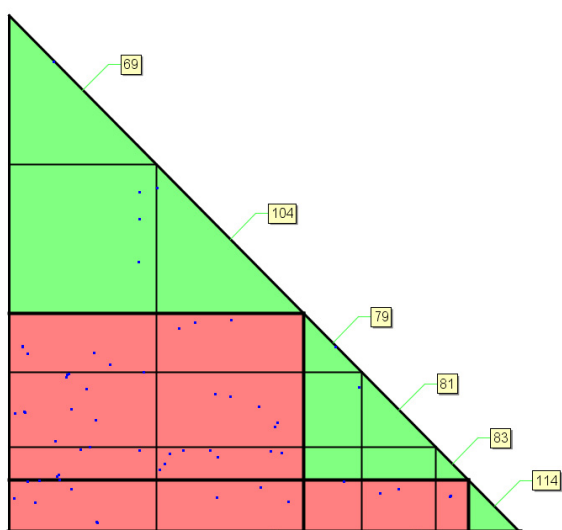
a

significance	gnathostome subgroup 1	gnathostome subgroup 2	gnathostome subgroup 3	gnathostome subgroup 4	gnathostome subgroup 5
1.59E-08	69,104	79,81,83	114		
1.19E-07	69,104	79,114	81,83		
1.26E-07	69,104	81,83	79	114	
1.74E-07	69,104	79,83	81	114	
2.29E-07	69,104	79,81	114	83	

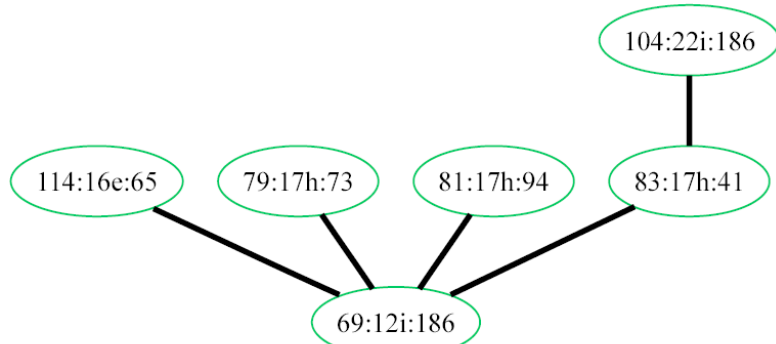
b

C

d



e



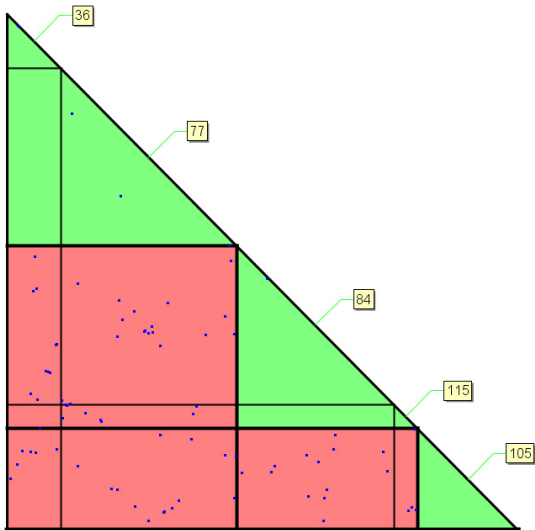
1

a

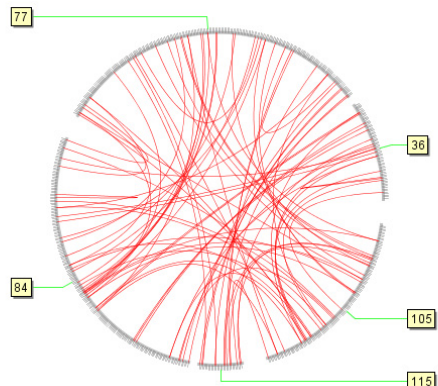
significance	gnathostome subgroup 1	gnathostome subgroup 2	gnathostome subgroup 3	gnathostome subgroup 4	gnathostome subgroup 5
4.77E-11	36.77	84.115	105		
9.50E-10	36.77	84	105	115	
6.81E-08	84.115	77	105	36	
9.01E-07	77	84	105	36	115
2.23E-06	77	84	105	36.115	

b

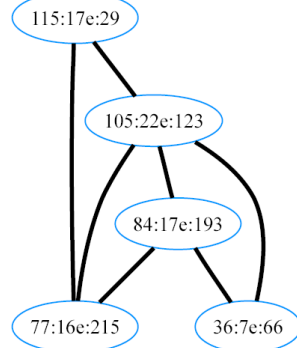
C



d



e



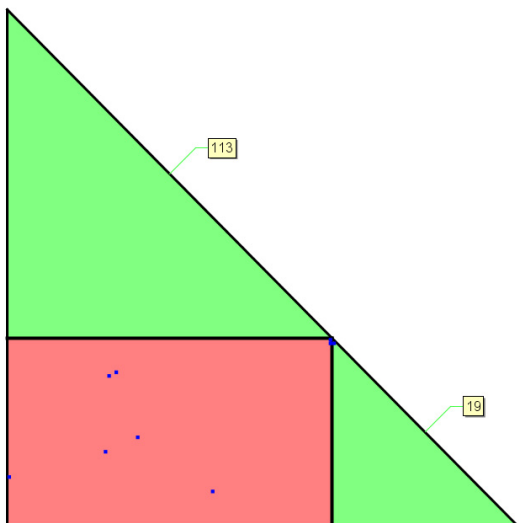
J

a

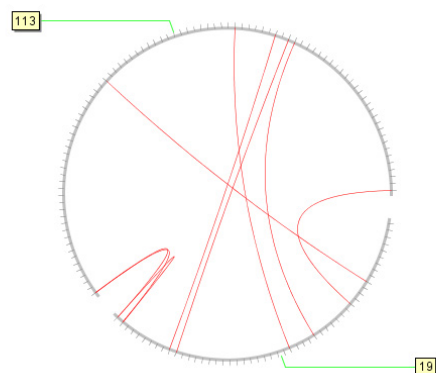
significance	gnathostome subgroup 1	gnathostome subgroup 2	gnathostome subgroup 3	gnathostome subgroup 4	gnathostome subgroup 5
0.011706765	113	19			

b

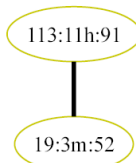
C



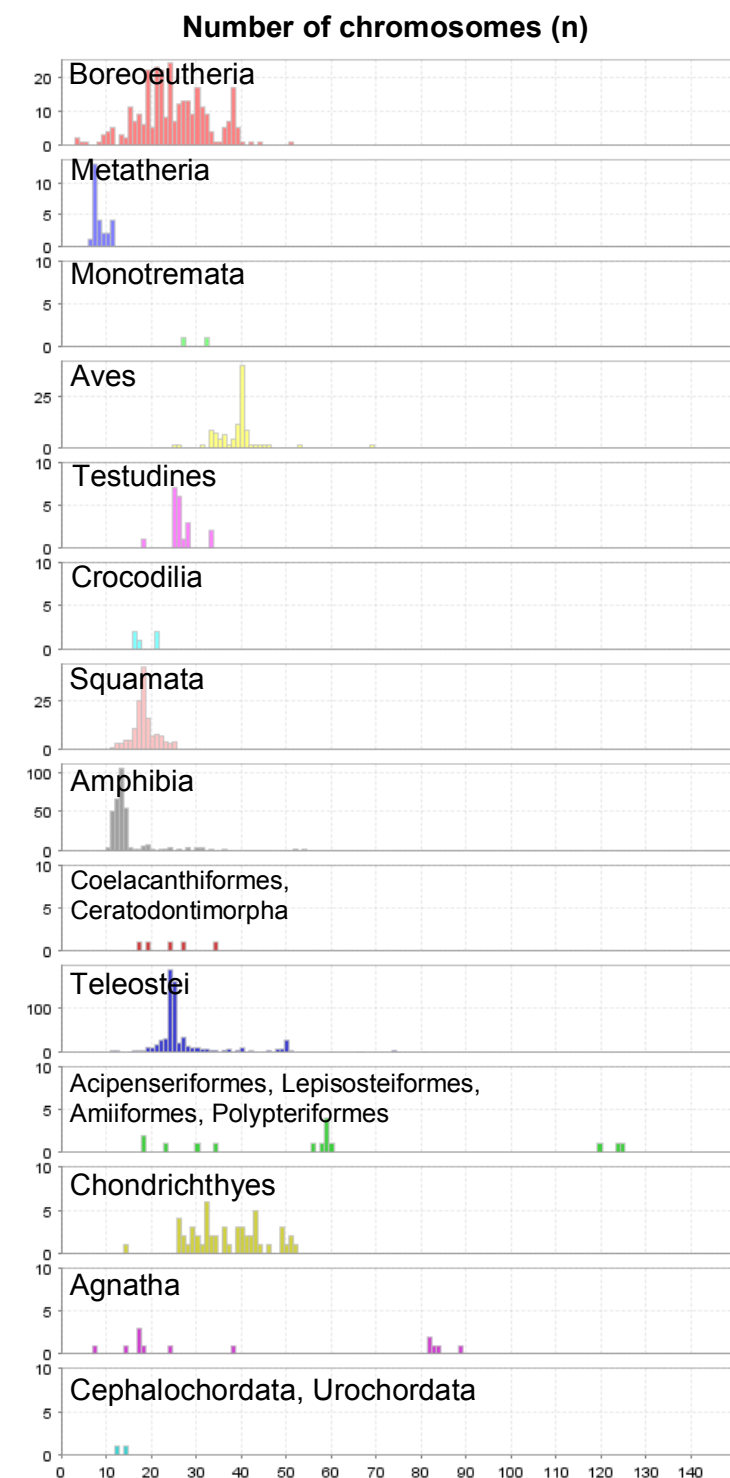
d



e

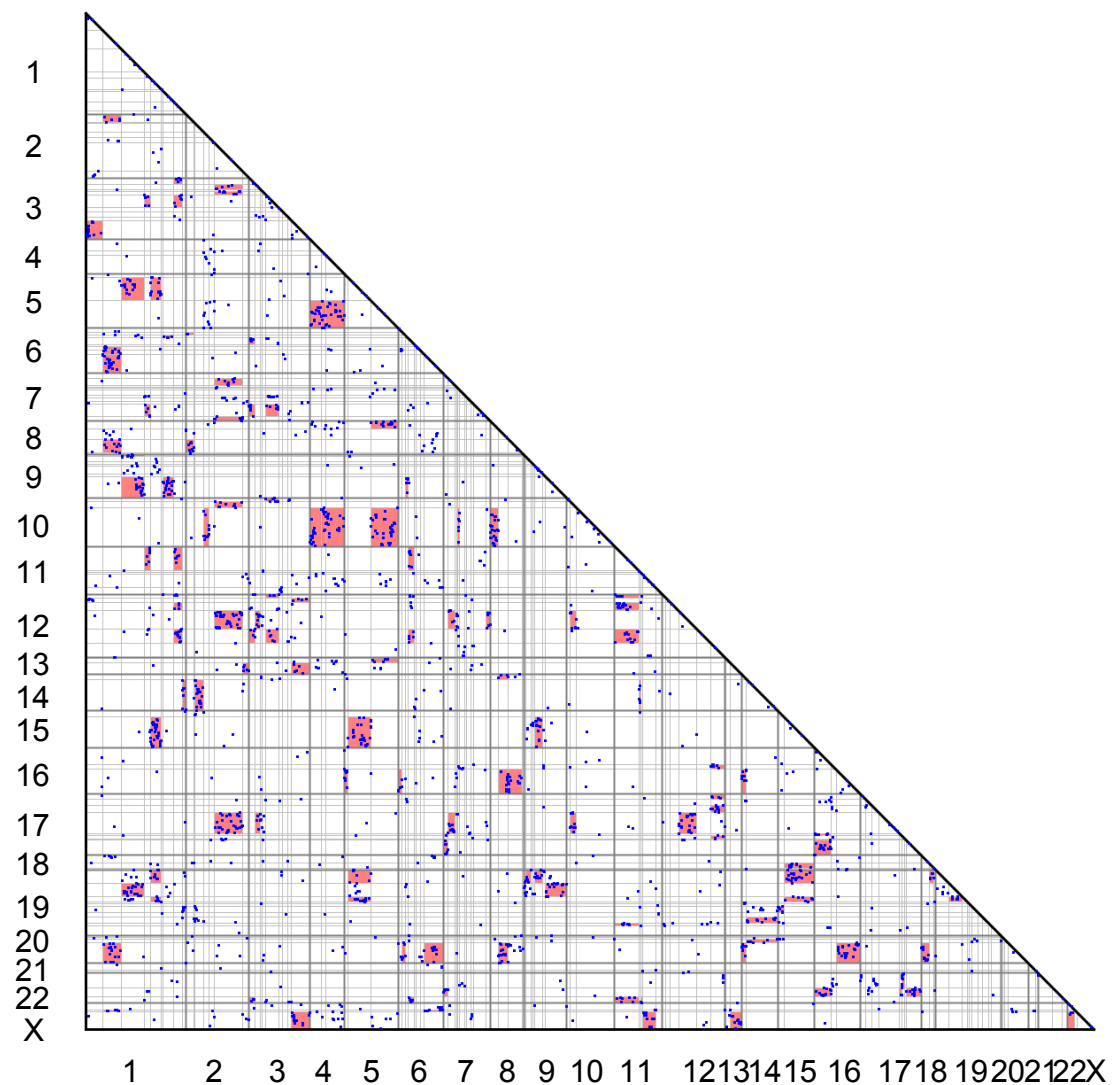


## Supplementary Figure S8



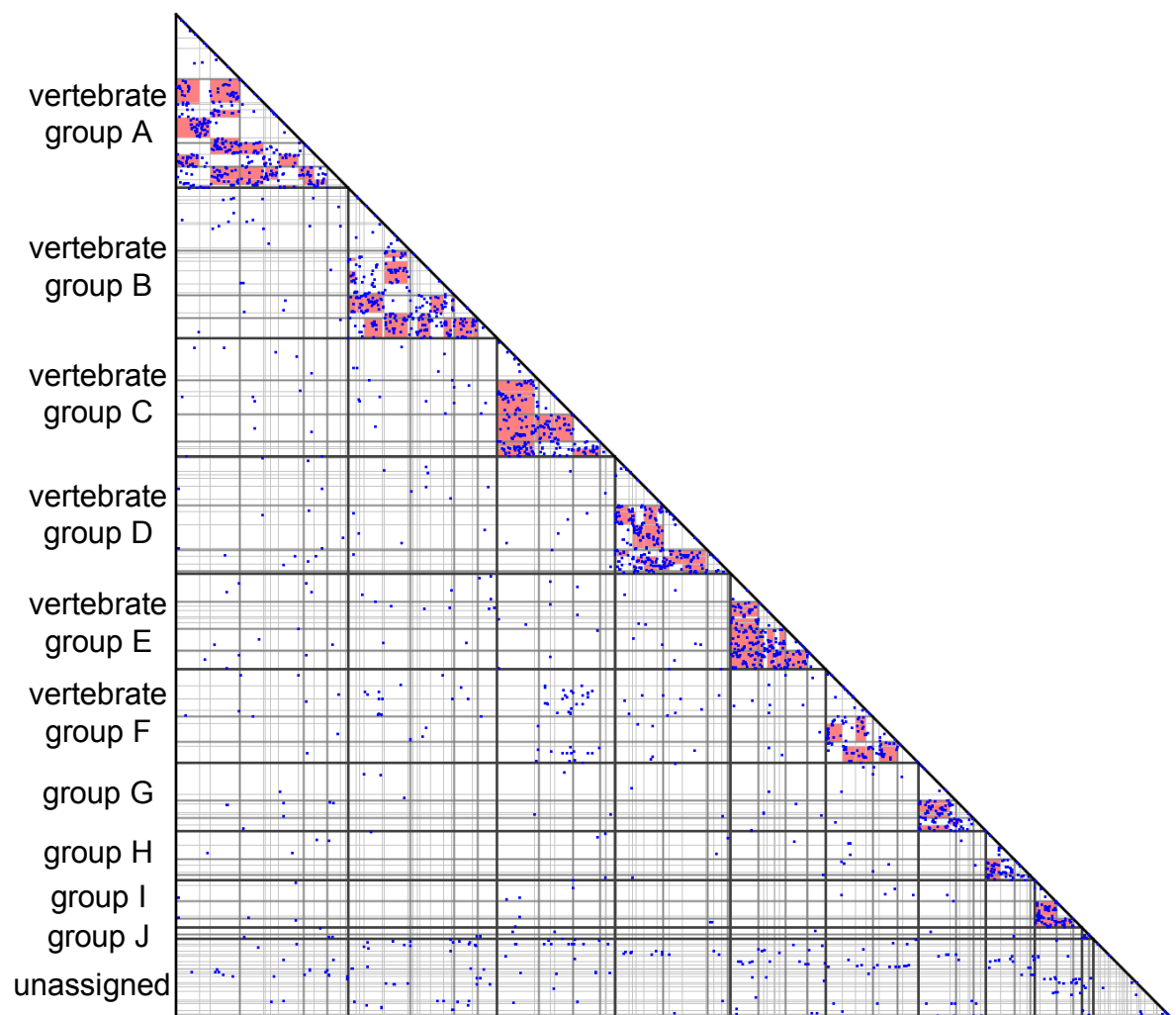
**Distribution of the number of chromosomes in individual lineages.** Some species possess additional lineage-specific whole-genome duplications.

**Supplementary Figure S9**



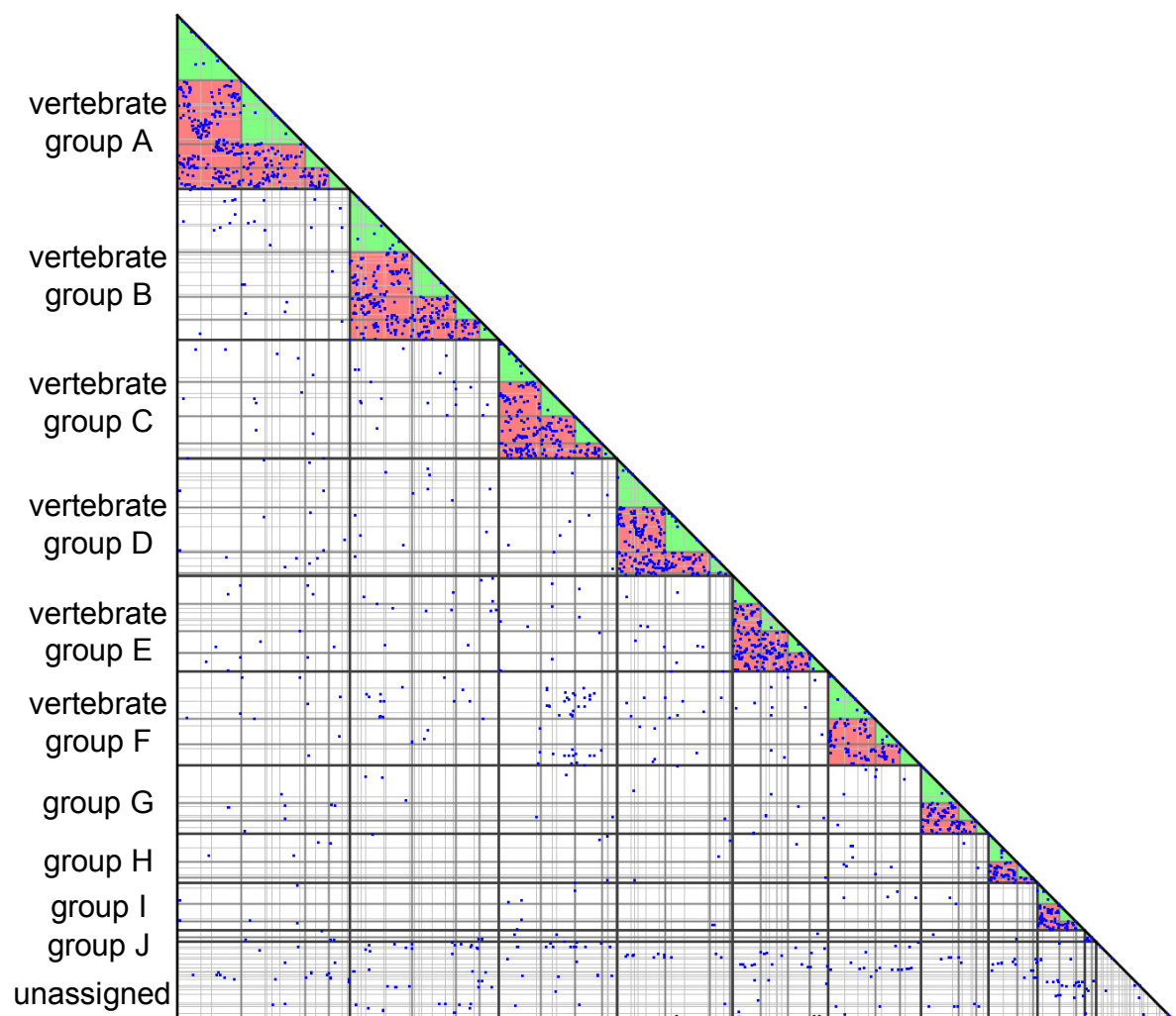
Enlarged copy of Fig. 2E.

**Supplementary Figure S10**



Enlarged copy of Fig. 2F.

**Supplementary Figure S11**



Enlarged copy of Fig. 2G.

## 10 Supplementary tables

## Supplementary Table S1

**CVL blocks in proto-chromosomes of the vertebrate ancestor.** Each CVL block in the proto-chromosome is associated with its identifier, the number of human genes, the number of human genes, the number of ohnologs, human chromosome, teleost ancestor chromosome, gnathostome ancestor chromosome, syntenic chicken chromosomes, and the total synteny block size for each chicken chromosome.

## Supplementary Table S2

## CVL blocks in proto-chromosomes of the osteichthyan ancestor.

### Supplementary Table S3

## CVL blocks in proto-chromosomes of the amniote ancestor.

**Supplementary Table S4****Effect of changing key parameter values on reconstruction of the vertebrate ancestral genome**

Case	1st parameter	2nd parameter	3rd parameter	Number of CVL blocks	Number of vertebrate groups	Number of quadruplicated vertebrate groups	Number of gnathostome subgroups	Number of osteichthyan proto-chromosomes	Number of amniote proto-chromosomes
1	10	1.E-04	1.E-02	118	10	5	34	31	26
2	7	1.E-04	1.E-02	139	9	6	32	28	24
3	13	1.E-04	1.E-02	105	10	4	35	28	26
4	10	5.E-04	1.E-02	118	9	6	32	31	26
5	10	5.E-05	1.E-02	118	10	5	34	30	26
6	10	1.E-04	5.E-02	121	9	5	31	28	25
7	10	1.E-04	1.E-03	114	10	6	35	30	25

1st parameter: the minimum threshold on the number of genes in a CVL block

2nd parameter: the maximum threshold on the significance (probability) that two CVL blocks are paralogous

3rd parameter: the maximum threshold for the Mann-Whitney U-test to decide whether a CVL block is divided

## 11 References

Benton, M.J. and Donoghue, P.C.J. 2007. Paleontological evidence to date the tree of Life. *Mol. Biol. Evol.* **24**: 26-53.

Blair, J.E. and Hedges, S.B. 2005. Molecular phylogeny and divergence times of deuterostome animals. *Mol. Biol. Evol.* **22**: 2275-2284.

Blomme, T., Vandepoele, K., De Bodt, S., Simillion, C., Maere, S., and Van de Peer, Y. 2006. The gain and loss of genes during 600 million years of vertebrate evolution. *Genome Biol.* **7**: R43.

Bourque, G., Zdobnov, E.M., Bork, P., Pevzner, P.A., and Tesler, G. 2005. Comparative architectures of mammalian and chicken genomes reveal highly variable rates of genomic rearrangements across different lineages. *Genome Res.* **15**: 98-110.

Crow, K.D., Stadler, P.F., Lynch, V.J., Amemiya, C., and Wagner, G.P. 2006. The "fish-specific" Hox cluster duplication is coincident with the origin of teleosts. *Mol. Biol. Evol.* **23**: 121-136.

Dehal, P. and Boore, J.L. 2005. Two rounds of whole genome duplication in the ancestral vertebrate. *PLoS Biol.* **3**: e314.

Dehal, P.S. and Boore, J.L. 2006. A phylogenomic gene cluster resource: the Phylogenetically Inferred Groups (PhIGs) database. *BMC Bioinformatics* **7**: 201.

Hedges, S.B. and Poling, L.L. 1999. A molecular phylogeny of reptiles. *Science* **283**: 998-1001.

Hoegg, S., Brinkmann, H., Taylor, J.S., and Meyer, A. 2004. Phylogenetic timing of the fish-specific genome duplication correlates with the diversification of teleost fish. *J. Mol. Evol.* **59**: 190-203.

Inoue, J.G., Miya, M., Venkatesh, B., and Nishida, M. 2005. The mitochondrial genome of Indonesian coelacanth *Latimeria menadoensis* (Sarcopterygii: Coelacanthiformes) and divergence time estimation between the two coelacanths. *Gene* **349**: 227-235.

Jaillon, O., Aury, J.M., Brunet, F., Petit, J.L., Stange-Thomann, N., Mauceli, E., Bouneau, L., Fischer, C., Ozouf-Costaz, C., Bernot, A. et al. 2004. Genome duplication in the teleost fish *Tetraodon nigroviridis* reveals the early vertebrate proto-karyotype. *Nature* **431**: 946-957.

Kellis, M., Birren, B.W., and Lander, E.S. 2004. Proof and evolutionary analysis of ancient genome duplication in the yeast *Saccharomyces cerevisiae*. *Nature* **428**: 617-624.

Kohn, M., Hogel, J., Vogel, W., Minich, P., Kehrer-Sawatzki, H., Graves, J.A., and Hameister, H. 2006. Reconstruction of a 450-My-old ancestral vertebrate protokaryotype. *Trends Genet.* **22**: 203-210.

Meyer, A. and Zardoya, R. 2003. Recent advances in the (molecular) phylogeny of vertebrates. *Annu. Rev. Ecol. Evol. S.* **34**: 311-338.

Naruse, K., Tanaka, M., Mita, K., Shima, A., Postlethwait, J., and Mitani, H. 2004. A medaka gene map: the trace of ancestral vertebrate proto-chromosomes revealed by comparative gene mapping. *Genome Res.* **14**: 820-828.

Postlethwait, J.H., Woods, I.G., Ngo-Hazelett, P., Yan, Y.L., Kelly, P.D., Chu, F., Huang, H., Hill-Force, A., and Talbot, W.S. 2000. Zebrafish comparative genomics and the origins of vertebrate chromosomes. *Genome Res.* **10**: 1890-1902.

Springer, M.S., Murphy, W.J., Eizirik, E., and O'Brien, S.J. 2003. Placental mammal diversification and the Cretaceous-Tertiary boundary. *Proc. Natl Acad. Sci. USA* **100**: 1056-1061.

Stadler, P.F., Fried, C., Prohaska, S.J., Bailey, W.J., Misof, B.Y., Ruddle, F.H., and Wagner, G.P. 2004. Evidence for independent Hox gene duplications in the hagfish lineage: a PCR-based gene inventory of *Eptatretus stoutii*. *Mol. Phylogenet. Evol.* **32**: 686-694.

Woodburne, M.O., Rich, T.H., and Springer, M.S. 2003. The evolution of tribospheny and the antiquity of mammalian clades. *Mol. Phylogenet. Evol.* **28**: 360-385.

Woods, I.G., Wilson, C., Friedlander, B., Chang, P., Reyes, D.K., Nix, R., Kelly, P.D., Chu, F., Postlethwait, J.H., and Talbot, W.S. 2005. The zebrafish gene map defines ancestral vertebrate chromosomes. *Genome Res.* **15**: 1307-1314.

Yamanoue, Y., Miya, M., Inoue, J.G., Matsuura, K., and Nishida, M. 2006. The mitochondrial genome of spotted green pufferfish *Tetraodon nigroviridis* (Teleostei: Tetraodontiformes) and divergence time estimation among model organisms in fishes. *Genes Genet. Syst.* **81**: 29-39.